

UCSF

UC San Francisco Electronic Theses and Dissertations

Title

Polycaprolactone thin film implants for glaucoma

Permalink

<https://escholarship.org/uc/item/3sc326vv>

Author

Kim, Jean

Publication Date

2017

Peer reviewed|Thesis/dissertation

Polycaprolactone thin film implants for glaucoma

by

Jean Kim

DISSERTATION

Submitted in partial satisfaction of the requirements for the degree of

DOCTOR OF PHILOSOPHY

in

Bioengineering

in the

GRADUATE DIVISION

of the

UNIVERSITY OF CALIFORNIA, SAN FRANCISCO

AND

Acknowledgments

Parts of this dissertation appear in full elsewhere or are in submission or preparation for publication in a peer-reviewed journal. Chapter 2 has been published in *Investigative Ophthalmology & Visual Science* 57:4341-4346 (2016) under the title “Biocompatibility and Pharmacokinetic Analysis of an Intracameral Polycaprolactone Drug Delivery Implant for Glaucoma” by Jean Kim, Max Kudisch, et al. Chapter 3 is in submission to a peer-reviewed journal and Chapter 4 and 5 are in the process of full manuscript preparation. Part of Chapter 4 was accepted to the 2017 Controlled Release Society Annual Meeting in the form of an abstract.

It was a great honor to be a part of the UC Berkeley-UCSF Graduate Program in Bioengineering and have the opportunity to work in the lab of Dr. Tejal Desai. I could not have asked for a more thoughtful and brilliant adviser than Tejal. I am incredibly thankful for the immense support she provided to my research and professional development. I also had the wonderful opportunity to work with the brightest of all- my lab mates in the Desai lab as well as colleagues at both UC Berkeley and UCSF. It was a privilege to become close friends with amazingly intelligent and kind people of the bay area. I also thank my collaborators in both academia and industry for providing their expertise and continuous support on my research. During earlier years in the graduate program, I went through a highly educational experience of preparing for my qualifying exam. I send my sincere thanks to my qualifying exam committee, including Drs. Jeffrey Lotz (committee chair), Dorian Liepmann, David Sretavan, and Deanna Kroetz, for our fruitful discussions before and during the qualifying exam. Also, I sincerely thank my dissertation mentors, Drs. Dorian Liepmann, Robert Bhisitkul, and my research adviser Tejal Desai, for the

helpful discussions and guidance throughout my research progress. Last but not least, none of my achievements would have been possible without the unconditional support of my family. My family always believed in me; their firm trust meant more than ever during the past 5 years.

Going through graduate school was certainly not an easy endeavor to say the very least. However, I feel overwhelmingly blessed to have the best people around me with their support and kind words whenever I was frustrated. My graduate research has been centered around the ultimate goal of seeing better. In addition to gaining extensive knowledge in ocular drug delivery and visual sciences, I learned to see the most important aspect in life- the privilege of being around those I truly love and respect.

Abstract

Glaucoma is a major leading cause of irreversible blindness. While glaucoma patients can greatly benefit from control of intraocular pressure (IOP) via hypotensive eye drops, physiological barriers and low patient compliance pose a great challenge to effective glaucoma therapy. Here, I present the development of a biodegradable intracameral implant that provides controlled release of a hypotensive agent for more than 6 months. The implant, made from polycaprolactone (PCL) and loaded with a hypotensive drug, was able to reduce IOP in normotensive rabbits for 23 weeks when implanted in the intracameral space. Evaluation of area under the curve of IOP measurements shows a significant difference in cumulative IOP reduction between eyes that received drug-loaded or empty device implantation. Furthermore, I demonstrate the potential of delivering two drugs with a single device as a means of long-term glaucoma combination therapy for patients who do not respond to monotherapy of hypotensive agent. Lastly, blends of low and high molecular weight PCL have been explored to achieve shorter time to fragmentation to tune degradation of PCL to meet the desired lifecycle of a glaucoma intracameral implant. In summary, the proof-of-concept drug delivery device shows promise as a potential mode of long-term glaucoma therapy based on its evaluation in vitro and in vivo.

Table of Contents

CHAPTER 1 – Introduction.....	1
1.1. Barriers to glaucoma treatment.....	2
1.1.1 Physiological barriers.....	2
1.1.2 Patient compliance.....	3
1.2 Existing formulation and drug delivery approaches	4
1.3 Benefits to controlled release in glaucoma management	5
CHAPTER 2 – Glaucoma implant optimization, in vitro evaluation, and short-term biocompatibility analysis in vivo	7
2.1 Abstract.....	8
2.2 Introduction.....	8
2.3 Materials and methods	10
2.3.1 Device fabrication.....	10
2.3.2 In vitro release studies and quantification analysis.....	11
2.3.3 In vivo device implantation	11
2.3.4 Analysis of drug distribution in rabbit ocular tissues	12
2.4 Results.....	13
2.5 Discussion.....	15
2.6 Conclusion	18
2.7 Acknowledgments.....	18
CHAPTER 3 – Long-term in vivo biocompatibility and pharmacokinetic, and pharmacodynamic analysis of PCL glaucoma implants	26
3.1 Abstract.....	27

3.2 Introduction.....	27
3.3 Materials and methods	29
3.3.1 Materials	29
3.3.2 Device fabrication and characterization.....	29
3.3.3 In vivo studies with loaded and empty device implantation	30
3.3.4 IOP measurements	31
3.3.5 Histological analysis.....	31
3.3.6 Quantification of DE-117 and hDE-117 in rabbit ocular tissues.....	32
3.3.7 Statistical analysis.....	32
3.4 Results.....	33
3.4.1 Device characterization before implantation and after euthanasia	33
3.4.2 Clinical evaluation of implanted PCL devices over 24 weeks	33
3.4.3 Drug distribution in ocular tissues.....	34
3.4.4 IOP following loaded or empty device implantation.....	35
3.4.5 Cumulative IOP reduction evaluated by AUC.....	36
3.4.6 Histological analysis after 24 weeks of device implantation.....	37
3.5 Discussion.....	38
3.6 Conclusion	40
3.7 Acknowledgments.....	41
CHAPTER 4 – Co-delivery of hypotensive agents using PCL implants.....	49
4.1 Abstract.....	50
4.2 Introduction.....	50
4.3 Materials and methods	51

4.3.1 Materials	51
4.3.2 Co-delivery device fabrication.....	51
4.3.3 In vitro drug release analysis	52
4.4 Results and discussion	53
4.5 Conclusion	54
CHAPTER 5 – PCL blending for intracameral implant applications.....	57
5.1 Abstract.....	58
5.2 Introduction.....	58
5.3 Materials and methods	61
5.3.1 Materials	61
5.3.2 PCL film fabrication and characterization.....	61
5.3.3 Gel permeation chromatography (GPC) analysis	62
5.3.4 Tensile testing.....	63
5.4 Results.....	63
5.4.1 Starting molecular weights of PCL blends	63
5.4.2 Molecular weight distribution of blends.....	64
5.4.3 Mechanical properties of blended film	64
5.5 Discussion.....	65
5.6 Conclusion	67
CHAPTER 6 – Summary and conclusions	73
References.....	76

List of Tables

Table 2.1 Summary of biocompatibility analysis	25
Table 5.1 Average molecular weights of unblended PCL comparing vendor-provided values and experimentally calculated values	71
Table 5.2 Mass ratios of PCL blending among low (10 kDa), medium (45 kDa), and high (80 kDa) PCL and the resulting M_n and M_w	72

List of Figures

Figure 2.1 Schematic diagram of device fabrication and photo of a PCL device	20
Figure 2.2 Release of hypotensive agent in vitro.....	21
Figure 2.3 Representative photos of rabbit eye after implantation of devices.....	22
Figure 2.4 Drug distribution in ocular tissues.....	23
Figure 2.5 Macroscopic photos of PCL devices collected from the rabbit eye	24
Figure 3.1 Representative ocular photo after device implantation	42
Figure 3.2 Drug distribution in ocular tissues with long-term device exposure.....	43
Figure 3.3 IOP change from baseline with loaded or empty device implantation.....	44
Figure 3.4 Long-term IOP fluctuation with device implantation	45
Figure 3.5 Cumulative IOP reduction.....	46
Figure 3.6 Histological analysis of the rabbit corneas.....	47
Figure 4.1 Schematic diagram of device fabrication and image of co-delivery device.....	55
Figure 4.2 Release of two hypotensive agents in vitro	56
Figure 5.1 Relationship between polystyrene standards' molecular weight and peak retention time	68
Figure 5.2 Molecular weight distribution of unblended and blended PCL.....	69
Figure 5.3 Evaluation of mechanical properties of PCL blends	70

Chapter 1 – Introduction

1.1 Barriers to glaucoma treatment

Glaucoma, one of the leading cause of irreversible blindness, is expected to influence 76 million people worldwide by 2020 and 111.8 million people by 2040 [1]. Glaucoma is a group of ocular disorder characterized by progressive optic neuropathy [2]. As intraocular pressure (IOP) is thought to be the only modifiable risk factor, glaucoma is commonly treated with one or more hypotensive eye drops to decrease IOP, administered by patients up to 3 times daily. Previous studies showed that reduction of IOP has substantial therapeutic benefit for glaucoma patients [3, 4] and reduction of 1 mmHg in IOP was linked with approximately 10% decreased risk of glaucoma progression [4]. However, there are barriers to glaucoma therapy stemming from its mode of administration.

1.1.1 Physiological barriers

Various physiological barriers to eye drops and ocular pharmacokinetic analysis of topical agents have been thoroughly reviewed in literature [5, 6]. To briefly describe, a topically administered therapeutic agent first meets the tear film, which turns over rapidly with mean turnover rate of 30% per minute [7]. Then the corneal epithelium, which lines the surface of the cornea, acts as a barrier because the superficial corneal epithelium is joined by tight junctional complexes that slow permeation of drugs. As a consequence, studies report that most (over 95%) topical ocular drugs are not absorbed by the target tissues in the inner eye [6]. Furthermore, drug that is cleared enters systemic circulation and may lead to systemic side effects [8, 9]. For example, timolol, which is a β -blocker used in the form of eye drops (timolol maleate ophthalmic solution) for

glaucoma therapy, may result in unintended cardiovascular effects due to the cleared drug entering systemic circulation [10]. Furthermore, the aqueous humor, which fills the anterior chamber and is in contact with target tissues for glaucoma, turns over relatively quickly with an average rate of 2.75 $\mu\text{L}/\text{min}$ in humans [11]. Assuming total anterior chamber volume of 202 μL [12], complete turnover is expected to take place in approximately 70 minutes. In other words, even if a drug bypasses many physiological barriers to reach the anterior chamber, it is likely cleared in less than two hours due to the convective turnover of the aqueous humor. Due to these physiological challenges, an intracameral device that can bypass the corneal barrier and provides constant release of drug in the anterior chamber has substantial potential to provide a more effective treatment than topical eye drops.

1.1.2 Patient compliance

While drug delivery through eye drops allows relatively convenient and minimally invasive mode of drug administration, the frequency of eye drops necessary for therapy poses a substantial burden on the patients. A multicenter study of compliance found that more than half of studied patients were not compliant to treatment or demonstrated improper technique using eye drops [13]. Furthermore, as age is one of the risk factors of glaucoma [14] and older age is associated with increased glaucoma progression [4], the use of eye droppers by the elderly should be carefully considered. Previous literature reports noted that glaucoma patients find it challenging to use eye droppers properly [15] (which can easily lead to over- or under-dosing) and that forgetfulness is one of the major causes of non-compliance [16]. A study that focused on assessing elderly medication adherence noted that 23% of elderly patients were non-adherent to

therapy with 112 mean number of days without therapy in a year [17]. It should be noted that since glaucoma results in an irreversible form of blindness, low adherence to therapy and subsequent reduced control over IOP is especially detrimental to the patients' quality of life. Several studies investigated the relationship between patients' quality of life and vision loss due to glaucoma [18, 19] and unsurprisingly, blindness was thought to have a substantial impact on the patients' quality of life. According to a national survey performed by the American Foundation for the Blind (AFB), severe vision loss ranked similar to paralysis regarding its negative impact on quality of life [20].

1.2 Existing formulation and drug delivery approaches

Recognizing the issues of physiological barriers and patient compliance in glaucoma therapy, substantial effort has been dedicated to developing a long-term therapy for glaucoma. For example, contact lenses have been explored as a drug delivery device for glaucoma [21-25]. Various methods such as imprinting [22], dispersion of nanoparticles in hydrogel [23], and incorporation of diffusion barrier [24] have been utilized to enhance drug loading as well as drug elution kinetics. Furthermore, mucoadhesive nanostructured microparticles [26-28] were explored to achieve greater preocular retention time and bioavailability of topically administered ocular drugs. This study showed that the nanostructured surface allowed microparticles to have much greater specific surface area, increasing adherence to the mucous layer of the eye [26]. Drug delivery using microneedles have also been extensively studied for ocular applications [29-33]. Among those, a recent study delivering polymeric particles through a microneedle via supraciliary route reported reduction in IOP in rabbits for one month [30].

1.3 Benefits to controlled release in glaucoma management

As noted earlier, several barriers to ocular drug delivery, such as physiological barriers and patient non-compliance, prevent effective glaucoma treatment. A device that can provide controlled (zero-order) release of a therapeutic agent for a prolonged period of time can be particularly beneficial for glaucoma. Because glaucoma is a chronic disease, patients may be expected to be under glaucoma medication for the remainder of their life; the burden of daily use of eye drops can be substantial for the patients. In addition, there are numerous reports on ocular surface toxicity that stems from repeated administration of eye drops [34-36]. Furthermore, because glaucoma results in an irreversible form of blindness, rigorous drug compliance followed by long-term drug non-compliance is unlikely to restore vision loss that resulted from inconsistent IOP control. An Advanced Glaucoma Intervention Study (AGIS) also noted long-term IOP fluctuation, the standard deviation of IOP at all visits, as a potential risk factor for visual field progression in patients with low mean IOP [37]. This suggests that long-term fluctuation in IOP, which may result due to intermittent compliance to IOP-reducing medication, may negatively impact therapeutic outcome in addition to the consequences of insufficient IOP reduction.

For these reasons, a long-term drug delivery device implanted in the anterior chamber, bypassing the lacrimal and corneal barriers, has the potential to effectively provide long-term IOP control without imposing the burden of daily compliance to the patients. Furthermore, because

intracameral dosage of a glaucoma agent can be noticeably lower than its topical dosage, potential side effects of the therapeutic agent may be reduced.

Chapter 2 – Glaucoma implant optimization, in vitro evaluation, and short-term biocompatibility analysis in vivo

2.1 Abstract

We developed polycaprolactone (PCL) implants that achieve zero-order release of a proprietary ocular hypotensive agent (DE-117) over 6 months in vitro. The release rates of DE-117-loaded PCL devices were tuned based on an established predictive model and confirmed by in vitro release studies. Devices containing DE-117 and empty devices were implanted intracamerally in normotensive rabbits for up to 8 weeks' duration. Devices were retrieved after rabbits were euthanized and evaluated for tissue adherence. The drug remaining in each device was analyzed by high performance liquid chromatography. Drug distribution in ocular tissues was measured by liquid chromatography coupled with a tandem mass spectrometry (LC/MS/MS). In vitro release of DE-117 showed zero-order release with a release rate of 0.5 $\mu\text{g}/\text{day}$ over 6 months.

Implantation in rabbit eyes demonstrated that the devices were well tolerated in the intracameral space. Quantification of DE-117 and hDE-117 (the hydrolyzed active form of DE-117) in ocular tissues (cornea, iris-ciliary body, aqueous humor, retina-choroid, and vitreous) indicated sustained release of DE-117 and its conversion to hDE-117 when released from the device.

Analysis of drug remaining in the device found that concentration of hDE-117 was below the limit of detection, indicating the encapsulated drug was protected from hydrolysis in the device.

Proof-of-concept PCL drug delivery devices containing DE-117 show promise as a long-term glaucoma treatment based on their zero-order drug release profile in vitro, biocompatibility in vivo, and effective distribution of released drug in relevant ocular tissues.

2.2 Introduction

As mentioned in Chapter 1, there is a great unmet need in glaucoma therapy considering the burden of daily patient compliance and the importance of IOP control in glaucoma management. Prostaglandin analogs are advantageous candidates for a drug delivery implant due to their high potency, which allows a small mass of loaded drug to last a long period of time. For example, the proprietary prostaglandin analog DE-117 will require a maximum desired release rate of 0.5 $\mu\text{g}/\text{day}$ in the anterior chamber based on previous studies [38, 39]. The low desired release rate enables further miniaturization of the device, reducing bulk that may come from loading large amounts of less potent drugs. Furthermore, DE-117 is a promising candidate since it has been shown to reduce intraocular pressure (IOP) at a lower dose (0.002% [wt/vol]) [38]) than other prostaglandin analogs, such as latanoprost (0.005% [wt/vol]) or bimatoprost (0.01% [wt/vol]). DE-117, which is converted to its active form (hDE-117) by hydrolysis, is a selective prostaglandin EP2 agonist. It has been shown to significantly decrease IOP in animal models upon topical administration [39] and also in a phase 2a clinical study with a daily dose of 0.002% (wt/vol) eye drops [38]. We developed an implantable DE-117 delivery device for treatment of glaucoma up to 6 months. Our proof-of-concept drug delivery device encapsulates DE-117 between two diffusion-limiting polycaprolactone (PCL) films. The biodegradable polyester PCL has been extensively used in drug delivery applications [40-44] and has previously established ocular biocompatibility [45]. Furthermore, a previous study supports the use of PCL films as a diffusion-limiting barrier for delivery of a highly hydrophobic drug, rapamycin, to the eye with zero-order release kinetics [40]. To assess the potential of a PCL device as a long-term intracameral implant, we investigated drug release in vitro, device biocompatibility in rabbit anterior chambers, distribution of DE-117 and its active form in rabbit ocular tissues, and analysis of remaining device payload after in vivo release.

2.3 Materials and methods

All chemicals were obtained from Sigma-Aldrich Corp. (St. Louis, MO, USA) unless noted otherwise. DE-117, its active form (hDE-117), and deuterium-labeled hDE-117 were prepared by Ube Industries, Ltd. (Ube, Japan). We obtained 10X stock PBS from Millipore (Billerica, MA, USA) and Tween 80 was obtained from Spectrum Chemical (New Brunswick, NJ, USA).

2.3.1 Device fabrication

We made PCL thin films by spin-casting. First, PCL ($M_n = 80$ kDa) was dissolved in 2,2,2-trifluoroethanol at a concentration of 150 mg/mL. Then, the solution was casted on a silicon wafer using a spin-coater (Specialty Coating Systems, Indianapolis, IN, USA) at 1000 rpm for 10 seconds. The casting process was repeated twice. Films were annealed at 110 °C to remove residual solvent and were left to cool at ambient temperature. Resulting films were thoroughly washed with Milli-Q deionized water and dried in air. Film thickness was measured using a film micrometer (iGaging, San Clemente, CA, USA). Four layers of PCL films were then stacked to create the desired thickness (224 μ m). Drug delivery devices were assembled by placing DE-117 powder between two stacked films and heat-sealing the edges [40]. Heat-sealing was performed with nichrome wire embedded in PDMS; PCL films were placed on the PDMS support above the wire and 1A current was applied to resistively heat the wire (Figure 2.1). The resulting devices were approximately 3 by 3 mm in dimension.

2.3.2 In vitro release studies and quantification analysis

All in vitro release studies used an elution buffer of PBS with 0.1% Tween 80 (pH 7.4). Devices (n = 4) were each submerged in 4 mL elution buffer. Volume of elution buffer was chosen to provide an absolute sink condition based on the solubility of DE-117 in buffer (25 µg/mL). The devices were placed on an orbital shaker at 120 rpm in a 37 °C incubator to mimic physiological conditions. For each sampling time point, the elution buffer was collected and replaced with fresh buffer. Concentration of DE-117 in the collected elution buffer was measured using high performance liquid chromatography (HPLC; 1260 Infinity Quaternary LC System, Agilent Technologies, Santa Clara, CA, USA). A C18 reverse-phase column (Eclipse Plus C18, 4.6 x 100 mm, 3.5 µm; Agilent Technologies) was used with a gradient of mobile phase A:B (65:35–45:55 in 12 minutes). Mobile phase A contained 0.03% trifluoroacetic acid in deionized water and mobile phase B was HPLC-grade acetonitrile (Thermo Fisher Scientific, Waltham, MA, USA). Detection was done at a wavelength of 260 nm. The release rate at each time point was calculated by dividing the amount of drug collected by the duration between two time points. The average release rate was calculated by applying a linear regression to the cumulative released DE-117 versus time. Data is presented as mean ± standard deviation.

2.3.3 In vivo device implantation

To evaluate the release rate of each device prior to implantation, in vitro release was studied for 10 days before implantation. Then, devices were collected, dried in a vacuum overnight, transferred to a sterile hood, washed in 70% ethanol, and subsequently dried before implantation.

Implantation of PCL devices in the rabbit eye was performed in accordance with the ARVO Statement for the Use of Animals in Ophthalmic and Vision Research. New Zealand white rabbits were premedicated with 0.03 mg/kg intramuscular buprenorphine and then anesthetized by inhalation of isoflurane (2–4%). Proparacaine hydrochloride (0.5%) ophthalmic drops were given as topical anesthetic followed by Betadine drops (5% povidone iodine solution). A clear corneal incision was then made using a 2.8-mm slit knife (Alcon Laboratories, Ft. Worth, TX, USA) and widened to 4 mm, through which the PCL device was inserted into the anterior chamber. The incision was closed with 7-0 polyglactin 910 suture (Vicryl; Ethicon, Somerville, NJ, USA). Surgical procedures were performed on one eye and the contralateral eye was untreated. Clinical ophthalmologic exams by visual inspection of non-anesthetized animals were performed at day 1, week 1, and 7 with anterior segment photography performed at all time points using a digital single-lens reflex (DSLR) camera (Canon EOS Rebel T4i; Canon USA, San Jose, CA, USA). Exams utilizing the operating microscope were also performed immediately after implantation as well as prior to euthanization and photos were taken with the Canon camera body and a SLR camera-microscope adapter (Carl Zeiss Meditec, Inc., Dublin, CA, USA).

2.3.4 Analysis of drug distribution in rabbit ocular tissues

Rabbits were anesthetized as described above and euthanized at various time points post-implantation (1, 2, 4, and 8 weeks) by intravenous injection of 2 mmol/kg potassium chloride into the marginal ear vein. The ocular globe was enucleated immediately after euthanasia. Aqueous humor was withdrawn by limbal paracentesis using a 30-gauge needle on a 1-mL

syringe. The globe was dissected to collect cornea, iris-ciliary body, retina-choroid, and vitreous humor, and preserved by freezing at -80°C . We extracted DE-117 and hDE-117 from aqueous humor and homogenates of vitreous humor, cornea, iris-ciliary body, and retina-choroid by addition of organic solvents. We determined DE-117 and hDE-117 concentrations in ocular tissues by a liquid chromatography coupled with a tandem mass spectrometry (LC/MS/MS) and calculated by the analytical concentration, tissue wet weight, and dilution factor. Deuterium-labeled hDE-117 was used for the internal standard of DE-117 and hDE-117 analyses. High performance liquid chromatographic system consists of system controller CBM-20A, solvent delivery unit LC30AD, auto-sampler SIL-30AC, and column oven CTO-30AC and degasser DGV-20A (Shimadzu Corp., Kyoto, Japan). An analytical column (Kinetex XB-C18, 2.1 x 50 mm inner diameter, 2.6 μm ; Phenomenex, Torrance, CA, USA) was used with a gradient of mobile phase A:B (68:32– 10:90). Mobile phase A contained 0.1% formic acid in deionized water and mobile phase B contained 0.1% formic acid in acetonitrile. The system (AB SCIEX QTRAP 5500; AB Sciex, Foster City, CA, USA) interfaced by turbo ion spray with positive ion source in multiple reaction monitoring mode was applied for detection. We used LC/MS grade of acetonitrile, methanol, and formic acid (Wako Pure Chemical Industries, Ltd., Osaka, Japan) throughout sample preparation and LC/MS/ MS analysis.

2.4 Results

Guided by a previously established model [46], the final device was made with PCL film that was 224 μm thick and approximately 3 by 3 mm in dimension (Figure 2.1). These DE-117-loaded PCL devices achieved a zero-order release rate of 0.53 $\mu\text{g}/\text{day}$ in vitro ($R^2 = 0.9995$ to

linear fit) over 6 months (Figure 2.2). To obtain pharmacokinetic characteristics and confirm biocompatibility of these devices in the intracameral space, devices were surgically implanted into the anterior chamber of normotensive rabbits (Figure 2.3). Pre-implantation in vitro release studies of these devices yielded a linear release rate of $0.435 \pm 0.075 \mu\text{g/day}$ ($R^2 = 0.989$ to linear fit). The difference in release rate is due to the variability in device surface area that results from fabricating the devices by hand. Empty PCL devices were also implanted as controls (Figure 2.3).

Devices with and without DE-117 were well tolerated in the anterior chamber (Table 2.1), with no incidence of infectious complications, uveitis, or cataract over 8 weeks. The most frequent ocular complications occurred during the implantation process related to surgical trauma. The scale of the rabbit eye being substantially smaller than the human eye, these devices fit tightly in the shallow anterior chamber, positioning in direct contact with both the posterior cornea and the iris. Iris bleeding and/or hyphema occurred in four out of nine procedures overall. However, as the surgical technique was tuned, the rate of surgical trauma was reduced from two out of three surgeries (first day of surgery) to two out of six surgeries (second day) during the course of this study.

LC-MS analysis of DE-117 and hDE-117 showed that devices released DE-117 in the eye as expected from the in vitro release studies; once released, DE-117 was readily converted to its active form (Figure 2.4). Furthermore, concentration of hDE-117 in the aqueous humor was maintained at a relatively steady level ($93 \pm 25 \text{ ng/mL}$) over the time course studied (Figure 2.4), indicating sustained release of DE-117 and conversion to hDE-117 in vivo. Concentration of

hDE-117 in the aqueous humor was also near the C_{\max} achieved by topical administration of 0.1% DE-117 solution (108 ± 23 ng/mL) [39]. Concentration of DE-117 and hDE-117 in the blood was below the limit of detection.

Devices showed some macroscopically observable tissue adherence upon removal from the rabbit eye (Figure 2.5). However, we noted that three out of four devices that experienced hemorrhage events during implantation (indicated with an asterisk) showed tissue adherence. All devices that underwent implantation without surgical complications lacked noticeable tissue adherence. This suggests that device tissue adherence is due to the surgical trauma, not due to the material properties of the device. Furthermore, LC-MS analysis of DE-117 and hDE-117 concentration in ocular tissues (Figure 2.4) confirmed that the tissue adherence did not have an observable effect on the release of DE-117 from the device.

2.5 Discussion

Poor patient compliance in topical glaucoma treatment has been repeatedly reported [13, 17]. To overcome this challenge, several drug delivery implants for glaucoma are in development. These include an implant device for delivery of latanoprost (Durasert; Pfizer, New York, NY, USA) and a sustained release formulation of bimatoprost currently in phase 3 clinical trials (NCT02250651; Allergan, Irvine, CA, USA). We explored biodegradable polymers and formulations that can achieve a release of DE-117 of 6 months or more in the anterior chamber and chose PCL as our device material. Compared with other polymers that have been utilized in glaucoma drug delivery devices such as poly(lactic-co-glycolic acid) [48], we noted that a slow

degradation rate of PCL is important to achieve zero-order release of the therapeutic over several months. Since the device acts as a diffusion-limiting barrier in our design, a hypothetical polymer that degrades completely in 6 months would not be able to deliver the therapeutic at a constant rate for 6 months. While PCL has been utilized in intravitreal [42, 43] and subretinal implants [44], PCL has not been widely utilized as intracameral implants for treatment of diseases, such as glaucoma. Biocompatibility of PCL and its degradation profile in the ocular space have been well characterized and our study supports previous reports that indicate that PCL is well tolerated in the eye [40, 45] and degrades slowly [42]. Based on the concentration of DE-117 detected in the aqueous humor, in vivo release rates can be estimated. Previous studies have noted two main mechanisms of drug clearance from the anterior chamber: by convective flow due to aqueous humor turnover and by uveal blood flow [5]. In our calculations, we assumed that the main mode of DE-117 clearance from the anterior chamber is due to aqueous humor turnover considering the rapid turnover rate (2.31 $\mu\text{L}/\text{min}$ in rabbits [49], indicating complete turnover of aqueous humor in approximately 90 minutes). Based on this number, rate of drug release could be calculated by the equation below.

$$R = C \times aq$$

where R is the in vivo release rate of drug, C is the concentration of DE-117 found in the aqueous humor, and aq is the rate of aqueous humor turnover. Consequently, the estimated in vivo release rate of DE-117 is $0.42 \pm 0.24 \mu\text{g}/\text{day}$, which is comparable to the pre-implantation in vitro release rate ($0.44 \pm 0.08 \mu\text{g}/\text{day}$). We expect the actual in vivo release rate to be higher due to uveal blood flow or additional clearance mechanisms that increase the rate of DE-117

clearance. An additional term that accounts for uveal blood flow was not utilized in this calculation, as we noted that an accurate prediction of in vivo release rate is not possible due to the natural variability of the aq value [49] used in the calculation. Due to the simplifying assumptions, the equation is intended to provide an estimate of in vivo release rate in the intracameral space instead of an accurate prediction. With the constraints of the equation in mind, this calculation suggests that the experimental conditions used in the in vitro release study resembled physiological conditions in the anterior chamber of the eye and in vitro release results can be used to estimate release in vivo.

There are a few limitations of this study that should be addressed. Current fabrication processes involve manual positioning of PCL films on the heat-sealing apparatus to achieve desired device dimensions, which can result in unintended variability. Limitations of our study also include small number of animals tested with device implantation. Since the study was focused on evaluating the biocompatibility of the device, the study was not designed to test the IOP reducing effect of released DE-117. Furthermore, considering the location of implantation, damage to the corneal endothelium is possible. However, as pharmacokinetic analysis required dissection of the rabbit eyes, histology could not be performed after euthanization to check for damages. Also, based on previous report studying degradation of PCL [50, 51], 80 kDa PCL can take up to 2 years to completely degrade in vivo. To ensure the device is not retained in the eye after full drug depletion, the degradation rate of PCL should be tuned to match the desired lifetime of a glaucoma implant. Due to the potency of DE-117, the desired maximum release rate of DE-117 in the intracameral space is $0.5 \mu\text{g}/\text{day}$, which only requires loading $90 \mu\text{g}$ of the drug for a 6-month release. In this study, we tested the smallest devices that could be reliably made via

manual fabrication. However, there is potential to further miniaturize device size and reduce release rate to match the dose that has been successfully tested in clinical trials (0.002% wt/vol daily eye drops) [38]. Upon device miniaturization, the position of device implantation can also be optimized so that the devices are away from the angle of the eye. Future studies will be powered to evaluate the IOP-reducing effect of intracameral implants containing DE-117 over 6 months. Also, histologic analysis on the effect of intracameral implantation will be performed to check corneal endothelial damage. Furthermore, study of these devices in larger animals, such as dogs or monkeys, will provide better representations of the IOP-reducing effect in humans. In addition, blends of PCL with other biodegradable polymers, such as poly(D,L-lactide) (PLA), can be explored to tune degradation rates. Previous studies have shown that the degradation rate of physical blends of PLA and PCL is between those of pure PLA and PCL [52].

2.6 Conclusion

In summary, we demonstrate the potential of DE-117 PCL devices based on in vitro release kinetics of DE-117, biocompatibility of device in the intracameral space, and distribution of DE-117 and hDE-117 in ocular tissues upon implantation. Future studies will focus on optimizing the devices and evaluating the major points described above for further development and clinical translation.

2.7 Acknowledgments

This work was supported by R01EY021574 from the National Institutes of Health, a research grant from Santen Pharmaceutical Co., Ltd., and an unrestricted grant from Research to Prevent Blindness. We thank Drs. Daniel Bernards and Kevin Lance for providing valuable comments during manuscript preparation.

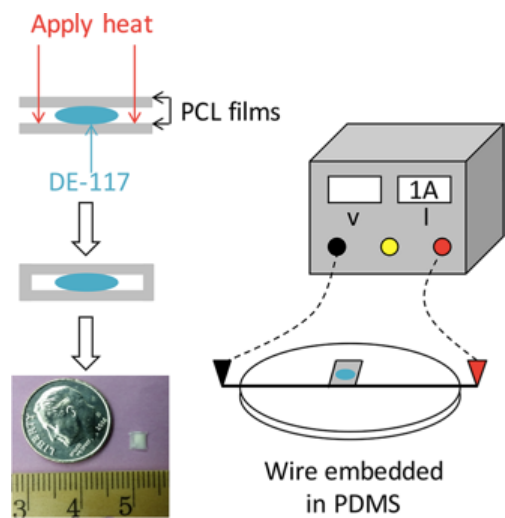


Figure 2.1 Schematic diagram of device fabrication and photo of a PCL device containing DE-117, with dime and metric ruler (millimeter tick marks) for scale. DE-117 was encapsulated between two PCL films and the edges of PCL films were heat-sealed by applying current to a wire embedded in PDMS.

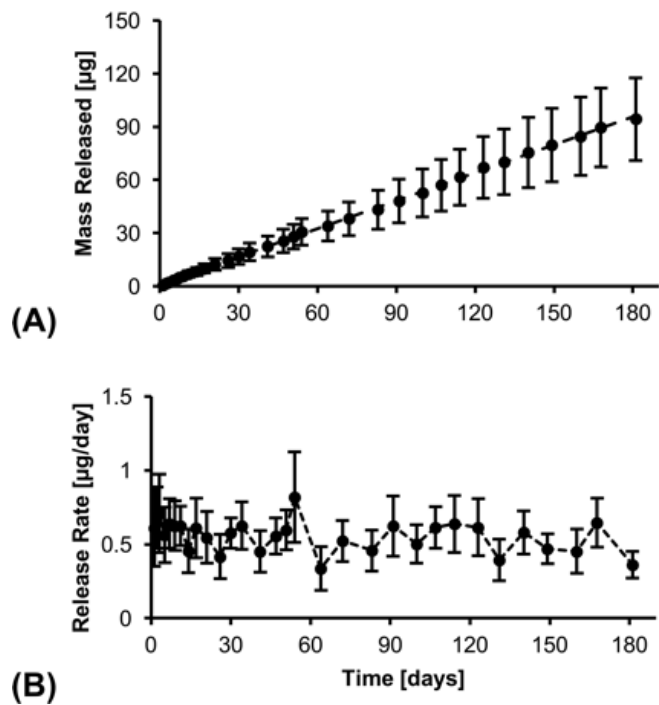


Figure 2.2 (A) Cumulative mass released and (B) release rate of DE-117 over 6 months in vitro.

Linear fit of cumulative mass released show zero-order release.



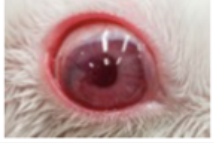
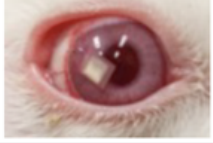

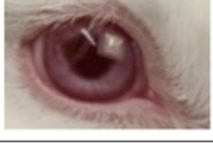
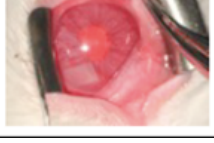

	Empty Device	Loaded Device
Day 1		
Week 1		
Week 7		
Week 8 (Sacrifice)		

Figure 2.3 Representative photos of rabbit eye after implantation of empty or DE-117 loaded drug delivery devices. Devices were well tolerated in the anterior chamber of rabbit eyes.

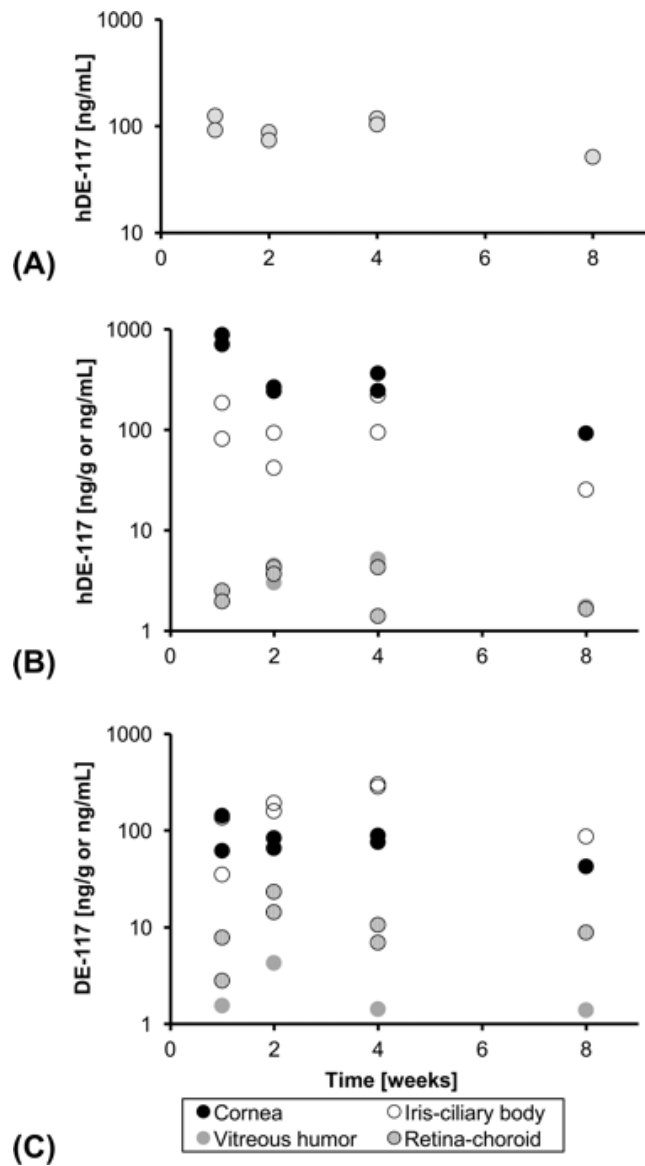


Figure 2.4 (A) Concentration of hDE-117 in the aqueous humor, distribution of (B) hDE-117 and (C) DE-117 in ocular tissues through 8 weeks after device implantation. Units are ng/ml for aqueous humor and vitreous humor and ng/g for cornea, iris-ciliary body and retina-choroid. Concentration of DE-117 and hDE-117 in ocular tissues shows sustained release of DE-117 in the anterior chamber and its conversion to hDE-117 upon release.

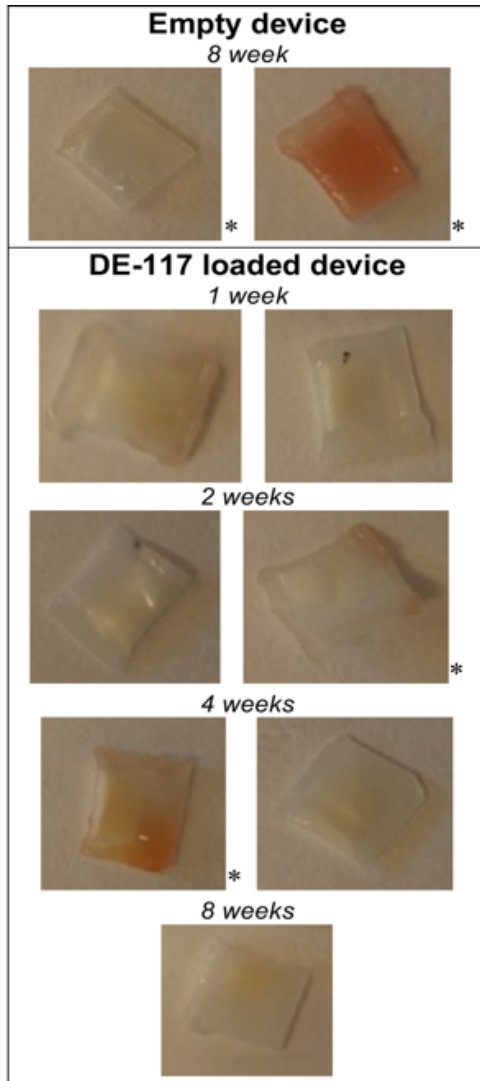


Figure 2.5 Macroscopic photos of PCL devices collected from the rabbit eye through 8 weeks, showing tissue adherence after residence in the intracameral space. A correlation between tissue adherence and hemorrhage events during implantation (noted by an asterisk) has been observed.

Table 2.1 Summary of biocompatibility analysis

	Empty device	Loaded device
Total number of implantation	2	7
Hyphema/Iris bleeding	2	2
Cataract formation	0	0
Inflammation	0	0

**Chapter 3 – Long-term in vivo biocompatibility and pharmacokinetic, and
pharmacodynamic analysis of PCL glaucoma implants**

3.1 Abstract

Long-term treatment of glaucoma, a major leading cause of blindness, is challenging due to poor patient compliance. Therefore, a drug delivery device that can achieve drug release over several months can be highly beneficial for glaucoma management. Here, we evaluate the long-term pharmacokinetics and therapeutic efficacy of polycaprolactone intracameral drug delivery devices in rabbit eyes. Our study showed that a single drug delivery device loaded with a proprietary hypotensive agent, DE-117, reduced intraocular pressure in normotensive rabbits significantly for 23 weeks. In addition, we demonstrated that concentration of DE-117 and its hydrolyzed active form (hDE-117) was maintained in the aqueous humor and the target tissue (iris-ciliary body) up to 24 weeks. Our proof-of-concept glaucoma implant shows potential as a long-term treatment that circumvents patient compliance barriers compared to current treatment via eye drops.

3.2 Introduction

We previously reported *in vitro* and short-term *in vivo* evaluation of an intracameral polycaprolactone (PCL) implant for glaucoma therapy that releases a proprietary hypotensive agent (DE-117) with zero-order release kinetics for up to 6 months *in vitro* [53]. DE-117 is a selective EP2 agonist when converted to its active form (hDE-117) by hydrolysis. Previous studies showed the hypotensive efficacy of topical DE-117 in animal models [39] and in a clinical trial [38]. DE-117 was chosen based on its high potency (0.002%) [38] compared to other glaucoma medications, which reduces the amount of payload necessary for a long-term (6-

month) implant [53]. We chose the intracameral space for our implant because the aqueous humor, which fills the intracameral space and serves as the drug elution medium for the implant, is in direct contact with the target tissue in the anterior segment of the eye. PCL, a biodegradable polyester that has been used as a diffusion-limiting barrier in our drug delivery device [40, 53], has been shown to have long-term biocompatibility in the eye [40, 45].

While ocular implants require more invasive insertion procedure compared to eye drops, a study in Singapore found that 62.8% of glaucoma patients were willing to accept a subconjunctival implant instead of eye drops [54]. In addition, a more recent study found that more than half of interviewed glaucoma patients were willing to accept intracameral drug administration for sustained drug delivery systems [55]. Implants may be able to provide better controlled release of drug over an extended period of time due to increased total amount of drug payload and easier control over the diffusive polymer barrier compared to drug delivery via particles. Supporting the potential of implants for glaucoma therapy, there are clinical trials evaluating drug delivery implants that aim to provide long-term treatments for glaucoma including bimatoprost sustained-release (NCT02250651) and ENV515 travoprost extended release (XR) (NCT02371746).

In this study, the IOP reducing effects and pharmacokinetics of DE-117-loaded devices were investigated for 23 and 24 weeks respectively in vivo. We show long-term reduction of IOP in normotensive rabbits upon implantation of a DE-117 loaded device compared to an empty device implantation or no treatment. We also demonstrate ocular tissue distribution of DE-117 and hDE-117 after 5, 12, and 24 weeks of implantation as well as histological analysis of eyes with 24 weeks of device exposure.

3.3 Materials and methods

3.3.1 Materials

Chemicals were obtained from Sigma-Aldrich Corporation (St. Louis, MO, USA) unless noted otherwise. PCL with $M_n = 80$ kDa (Sigma-Aldrich Corporation) was used for device fabrication throughout the study. DE-117, its active form (hDE-117), and deuterium-labeled hDE-117 was prepared by Ube Industries, Ltd. (Ube, Japan).

3.3.2 Device fabrication and characterization

Devices were fabricated and evaluated as previously described [53] with minor modifications. To briefly describe, DE-117 powder was encapsulated between stacked PCL thin films, which were made by spin-casting. The edges of the devices were sealed by placing the device on a nichrome wire embedded in PDMS and resistively heating the wire. Devices were slightly miniaturized in both dimensions (approximately 2.5 to 3 mm in width and length) and film thickness (45 μm films stacked 4 times, resulting in 180 μm in thickness) compared to previous devices. Devices underwent in vitro release studies in 1 mL of phosphate-buffered saline (PBS: EMD Millipore, Billerica, MA, USA) with 0.1% Tween 80 (Spectrum Chemical, New Brunswick, NJ, USA) for 10 days before implantation. Release buffer was replaced with fresh buffer every two days. Concentration of DE-117 was measured using high performance liquid chromatography (HPLC) (1260 Infinity Quaternary LC System, Agilent Technologies, Santa

Clara, CA, USA) with a gradient of mobile phase A:B = 90:10 to 20:80 in 40 minutes (A = deionized water with 0.03% trifluoroacetic acid and B = HPLC grade acetonitrile (Thermo Fisher Scientific, Waltham, MA, USA)).

3.3.3 In vivo studies with loaded and empty device implantation

Implantation of PCL devices in the rabbit eye was performed in accordance with the ARVO Statement for the Use of Animals in Ophthalmic and Vision Research (1995). PCL devices were implanted in New Zealand white rabbits as previously described [53] with minor adjustments. A 3.0 mm slit knife (Alcon Laboratories, Ft. Worth, TX, USA) was used to construct a clear corneal incision to insert the device in the anterior chamber. The incision was closed with 9-0 nylon suture (Alcon Laboratories, Ft. Worth, TX, USA). Surgical procedures were performed under sterile conditions on one eye of each animal and the other eye was kept untreated. Twelve rabbits were implanted with DE-117 loaded devices (euthanized after 5, 12, and 24 weeks, n=4 each) and 4 rabbits were implanted with empty devices as controls (euthanized after 24 weeks).

Clinical ophthalmologic exams of unanesthetized animals were performed after the surgery along with IOP measurements. Exams utilizing the operating microscope were performed immediately after implantation as well as prior to euthanasia and eye photos were taken with a Canon EOS Rebel T4i DSLR (Canon U.S.A, San Jose, CA, USA) camera body and a Zeiss SLR camera-microscope adapter (Carl Zeiss Meditec Inc., Dublin, CA, USA).

Rabbits were anesthetized and euthanized at the above time points post-implantation by intravenous injection of 2 mmol/kg potassium chloride into the marginal ear vein. Aqueous humor was withdrawn prior to euthanasia by limbal paracentesis using a 30-gauge needle on a 1 mL syringe. Blood samples were collected prior to euthanasia in tubes containing EDTA (BD Vacutainer®, BD, Franklin Lakes, NJ, USA) and kept on ice until centrifugation. Whole blood was centrifuged at 1300 x g for 15 minutes in a refrigerated centrifuge to separate cells from the sample. Eyes implanted with drug-loaded devices were enucleated, frozen in dry ice, and stored in -80 °C until dissection and analysis.

3.3.4 IOP measurements

IOP measurements were taken with a handheld rebound tonometer (TonoVet®, Icare, Helsinki, Finland) with three technical replicate measurements per eye between 11 am and 5 pm with the exception of one time point (measured once per eye due to logistical difficulties). Baseline IOP of rabbits dedicated to the 24-week time point were measured one day before the implantation procedure between 12 to 2 pm. Area under the curve (AUC) of baseline subtracted IOP values was calculated using the trapezoid rule.

3.3.5 Histological analysis

Eyes of rabbits with empty device implantation were enucleated immediately after euthanasia and submerged in 60 mL of Hartman's Fixative. After one day, globes were transferred to PBS (UCSF Cell Culture Facility, San Francisco, CA, USA) for two days and to 70% ethanol until

histological analysis. Histological preparation was performed by the Gladstone Histology and Light Microscopy Core (San Francisco, CA, USA). Eyes were cut longitudinally along a plane passing through the center of the cornea and the optic nerve and each half globe was processed, embedded, sectioned, and stained with hematoxylin and eosin (H&E). Images of the sectioned samples were taken with a brightfield microscope equipped with a Nikon DS-Ri2 camera and a Plan Apo 20x/0.75 objective at the Nikon Imaging Center (UCSF, San Francisco, CA, USA).

3.3.6 Quantification of DE-117 and hDE-117 in rabbit ocular tissues

Concentration of DE-117 and hDE-117 in dissected ocular tissues was measured by liquid chromatography coupled with a tandem mass spectrometry (LC/MS/MS) as previously described [53]. One vitreous sample (5-week time point) was experimentally lost during sample preparation. After tissue dissection, drug delivery devices were retrieved and their residual drug (DE-117) payload was analyzed via ultra performance liquid chromatography (UPLC) (ACQUITY UPLC, Waters, Milford, MA, USA) with a gradient of mobile phase A:B = 100:0 to 10:90 in 4 minutes (A = deionized water with 0.03% trifluoroacetic acid/acetonitrile (9:1) and B = deionized water with 0.03% trifluoroacetic acid/acetonitrile (1:4)).

3.3.7 Statistical analysis

Statistical analysis was performed using Prism 7 (GraphPad Software, Inc., La Jolla, CA, USA). Repeated-measures analysis of variance (ANOVA) was used to determine statistical significance of baseline-subtracted IOP measurements between treated eyes and contralateral untreated eyes

over time. Two-tailed student's t-test with Bonferroni correction (number of comparisons = 3) and one-way ANOVA were used to evaluate statistically significant differences among AUC. Data is presented as mean \pm standard deviation.

3.4 Results

3.4.1 Device characterization before implantation and after euthanasia

In vitro release studies of devices were performed before implantation to confirm their release rates. The analysis showed that the implanted devices released DE-117 at a rate of 0.49 ± 0.11 $\mu\text{g}/\text{day}$ (n=12, linear regression, R^2 ranging from 0.98 to 1.00 for each device), which was consistent with our previous study [53]. Remaining drug payload in the retrieved devices after euthanasia was also analyzed. While DE-117 was detected in the remaining drug payload, hDE-117 was not detected. This showed that DE-117 was protected from hydrolysis inside the device.

3.4.2 Clinical evaluation of implanted PCL devices over 24 weeks

The devices were generally well-tolerated in the intracameral space (Figure 3.1). There were no cataract formation or obvious signs of ocular inflammation. We have previously reported a relatively high rate (4 out of 9) of iatrogenic iris trauma and/or hyphema during implantation procedures [53]. In this study, the rate of iris trauma and/or hyphema was reduced to 3 out of 16. In the previous work, we also noted the possibility of the device being stuck at the anterior chamber angle (between the root of the iris and the peripheral cornea [2]) [53]. Since the

trabecular meshwork located in the angle is the site of aqueous humor outflow [2], device migration to this location is generally not preferred. In this study, one device (drug loaded device implantation, euthanized after 12 weeks) migrated to the angle of the eye. However, device migration did not have an observable effect on device biocompatibility in the intracameral space. Of the 16 rabbits, one rabbit (empty device implantation, euthanized after 24 weeks) developed partial corneal opacification and neovascularization in the treated eye. This eye underwent histological analysis to assess potential corneal damage. Also, one case of transient subconjunctival hemorrhage was observed in a device implanted eye.

3.4.3 Drug distribution in ocular tissues

Concentration of DE-117 and hDE-117 was measured in the aqueous humor, vitreous, and iris-ciliary body of device implanted eyes (Figure 3.2). Concentration of DE-117 in the aqueous humor (Figure 3.2.A) indicated sustained release of DE-117 in the anterior chamber through 24 weeks. In addition, a previous study on in vitro hydrolysis of latanoprost (a prostaglandin analog prodrug used for glaucoma treatment) reported that conversion of latanoprost to its active form may be limited in the aqueous humor compared to conversion in other ocular tissues, such as the cornea and the ciliary body [56]. Because conversion of DE-117 to hDE-117 is important for its therapeutic effect, we wanted to confirm that DE-117 is sufficiently hydrolyzed to hDE-117 in the aqueous humor. Our analysis showed a concentration of hDE-117 in the aqueous humor (Figure 3.2.B) similar to that of DE-117 (Figure 3.2.A), indicating conversion of released DE-117 to hDE-117 in the aqueous humor up to 24 weeks after implantation. Concentration of hDE-117 in the vitreous humor was noticeably lower than that in the aqueous humor (Figure 3.2.B),

which is expected based on the location of device placement. DE-117 in the vitreous humor was below the limit of quantification. Both DE-117 and hDE-117 concentration in the target tissue (iris-ciliary body) was maintained at a relatively steady level at all time points (Figure 3.2.C,D). Considering the relatively small device variation characterized by pre-implantation in vitro release studies, variations in tissue drug concentrations are expected to be due to difference among each animal.

In addition, concentration of DE-117 and hDE-117 in the aqueous humor of untreated eyes was measured to check if the released drug can cross over to the contralateral eye. Analysis indicated that DE-117 and hDE-117 concentration in the aqueous humor of untreated eyes was below the limit of quantification (0.100 ng/mL). DE-117 and hDE-117 were also below the limit of quantification in the blood samples.

3.4.4 IOP following loaded or empty device implantation

IOP measurements of the device implanted eyes were compared to those of untreated, contralateral eyes for approximately 23 weeks after treatment (Figure 3.3.A,B). One week after implantations, IOP was reduced 7.1 ± 1.8 mmHg from baseline with DE-117-loaded devices while the contralateral eyes experienced an IOP reduction of 0.3 ± 2.9 mmHg. When averaging over all IOP measurements after implantation, loaded device implanted eyes experienced a -4.6 mmHg change in IOP while the contralateral eyes experienced a 0.3 mmHg change (repeated-measures ANOVA, $p < 0.005$). To evaluate the effect of device implantation independent of the effects of released drug, IOP was evaluated with empty device implantation (Figure 3.3.B).

Empty device implanted eyes did not experience measurable IOP reduction 6 days after the implantation procedure (change of 0.3 ± 1.7 mmHg) compared to contralateral eyes (0.2 ± 1.1 mmHg). However, when considering an average over all IOP measurements, empty device implantation did slightly lower IOP over time (-1.7 mmHg) compared to untreated eyes (0.1 mmHg) (repeated-measures ANOVA, $p < 0.05$), although to a lesser degree than eyes with drug-loaded devices.

In addition, a previous study evaluated the relationship between IOP fluctuation to visual field progression and concluded that long-term IOP fluctuation is linked with visual field progression in glaucoma patients with low mean IOP [37]. In this study, long-term IOP fluctuation was defined as the standard deviation of IOP in mmHg at all time points [37]. Following this observation, we evaluated the long-term IOP fluctuation in our study using the standard deviation of all IOP measurements after the implantation procedure. Lack of noticeable difference in long-term IOP variation was observed across all experimental groups (Figure 3.4).

3.4.5 Cumulative IOP reduction evaluated by AUC

Cumulative IOP reduction upon device implantation was evaluated by the AUC of IOP measurements from baseline. There was one-day difference in final IOP measurements between experimental groups (162 days for drug-loaded devices versus 161 days for empty devices), which will affect the precise AUC value. However, when normalized to the overall duration, the magnitude of the trend is largely unaffected, so the AUC values were compared without accounting for this effect. Furthermore, while most time points were measured weekly on the

same day of the week, some time points were adjusted to accommodate unavailability throughout the long-term evaluation; this sampling variability was accounted for during integration. Specific time points of IOP measurements are as shown in Figure 3.3. With these caveats in mind, there was a statistically significant difference for IOP AUC among loaded device implants, empty device implants, and untreated eyes (ANOVA, $p < 0.001$) (Figure 3.5). AUC upon drug-loaded device implantation was significantly greater than that with empty device implantation (two-tailed t-test with Bonferroni correction, $p < 0.05$) (Figure 3.5). Also, AUC of treated eyes was significantly different compared to that of untreated contralateral eyes for drug-loaded implantation ($p < 0.05$) but not with empty device implantation ($p > 0.05$) (Figure 3.5).

3.4.6 Histological analysis after 24 weeks of device implantation

Device-implanted eyes (without drug) and their contralateral (control, unimplanted) eyes (total 8 eyes) underwent histological analysis after 24 weeks of implantation. As corneal opacification and neovascularization were observed clinically in one of the implanted eyes, histological evidence of corneal damage was assessed. The eye with clinical corneal opacification and neovascularization exhibited a relatively thick layer of proteinaceous exudate, which appeared as an eosinophilic deposit, on the posterior corneal surface (black arrow in Figure 3.6.A).

Furthermore, this eye showed anterior synechia, adhesions between the anterior iris surface and the posterior cornea (Figure 3.6.B, white asterisk). The cause of anterior synechia is postulated to be of mechanical nature, as the implanted device pushed the iris against the cornea. In regions of anterior synechia, localized disruption of the corneal endothelium and presence of inflammatory cells in the corneal stroma were noted (white arrows in Figure 3.6.B). These histological findings

correlate with the clinically apparent partial corneal opacification and neovascularization (white arrowhead in Figure 3.6.B). Accumulation of exudate and inflammatory cells was either noticeably less or not present in other device-implanted eyes (Figure 3.6.C) and untreated eyes (Figure 3.6.D) and the corneal endothelium of those eyes generally appeared to be healthy (dotted black arrow in Figure 3.6.C,D). One device-implanted eye showed evidence of corneal endothelial metaplasia (dotted white arrow in Figure 3.6.E), which refers to the change of corneal endothelial cells to a fibrocyte phenotype. Corneal endothelial metaplasia is likely a long-term consequence of exudate accumulation below the cornea.

3.5 Discussion

Though glaucoma patients can greatly benefit from IOP control using hypotensive eye drops [3, 4], barriers to patient compliance pose a great challenge in efficacious glaucoma treatment. Furthermore, hypotensive eye drops must overcome ocular physiological barriers to reach the target sites. For example, once a drug is topically administered, it is cleared from the ocular surface via the lacrimal fluid flow and systemic absorption [5]. Then, the drug needs to pass through the cornea, which is lined with corneal epithelial cells. Surface corneal epithelial cells, joined by tight junctional complexes, act as a barrier for drug permeation [57]. Also, transporters expressed in the corneal epithelium may further influence drug absorption [57]. For these reasons, anterior tissue concentration of a topically administered drug is typically expected to be orders of magnitude lower than the eye drop concentration [5, 58]. Finally, ocular surface toxicity can arise with long-term use of various topical glaucoma medications [34-36]. A long-term intracameral drug delivery implant can be substantially beneficial for glaucoma treatment

because it requires minimal patient intervention after the implant is administered. In addition, when delivered from an intracameral implant, the therapeutic agent bypasses the corneal and lacrimal barriers to reach the target tissues.

We previously presented a PCL reservoir drug delivery device designed for the intracameral space [53]. The devices were able to deliver DE-117, a proprietary hypotensive agent, with controlled release kinetics over 6 months in vitro. In this study, we investigated the long-term in vivo efficacy of the devices for glaucoma treatment. IOP measurements showed that DE-117 loaded devices are able to provide a persistent IOP drop up to approximately 23 weeks. While we observed that empty device implantation also reduced IOP compared to non-implanted contralateral eyes over the studied period, cumulative IOP reduction with drug-loaded devices was significantly greater than that with either an empty device or no treatment. We hypothesized that the surgical procedure, post-operative healing, and/or mechanical effects may have played a role in IOP reduction with empty device implantation.

While this study demonstrates promising IOP reduction with DE-117 releasing implants, there are some limitations that should be noted. First, there is concern in implanting a bulky device in the anterior chamber that may potentially damage the corneal endothelium. For example, we noted one case of partial corneal opacification and neovascularization, which may have resulted due to endothelial damage during device insertion. Since the effect of PCL on corneal endothelial cell viability has been shown to be negligible compared to cells grown on a culture plate [41], we expect that the corneal endothelial damage is due to the surgical procedure or mechanical effects rather than the material (PCL). While the incidence of this complication was

noticeably low (one of 16 surgeries in this study), the rabbit corneal endothelium is known to have more regenerative potential than that of human [59]. Other animal models that better mimic the human cornea should be explored in the future, including cats [59] and non-human primates [60].

Moreover, we observed one case of device migration to the angle of the eye. Though device migration did not have an obvious effect on device biocompatibility, it resulted in lower drug distribution in ocular tissues than expected. To prevent device migration, device size may be reduced so that the device implantation site can be optimized. Furthermore, reduction in device size can allow device insertion through a smaller corneal incision, which may result in less IOP change upon empty device implantation. A smaller device may also reduce the incidence of anterior synechia since we suspect that the bulky proof-of-concept device can push the iris against the cornea, causing iris adherence to the cornea. In addition, a more thorough evaluation of ocular inflammation using standardized grading scales will be beneficial in future studies to validate the lack of apparent ocular inflammation observed in the clinical assessments of this study.

3.6 Conclusion

In summary, long-term biocompatibility and IOP reducing efficacy of the devices in vivo support the potential of our prototype intracameral implants for glaucoma therapy. In addition, analysis of drug distribution in ocular tissues showed that DE-117 and hDE-117 concentration was maintained up to 24 weeks in both the aqueous humor and the iris-ciliary body. With further

optimization of device shape and thorough testing in larger animals, the intracameral drug delivery devices may provide a new mode of glaucoma therapy that eliminates the heavy burden of daily patient compliance.

3.7 Acknowledgments

This work was partially supported by R01EY021574 from the National Institutes of Health (NIH), a research grant from Santen Pharmaceutical Co., Ltd., and the Mary Anne Koda-Kimble seed award. The laboratory for in vivo studies was supported by an unrestricted grant from Research to Prevent Blindness, a NIH/NEI Core Grant (EY002162), and That Man May See foundation. We thank Dr. Daniel A. Bernards, who provided valuable feedback and assistance on manuscript preparation, and the Nikon Imaging Center at UCSF for their imaging support.

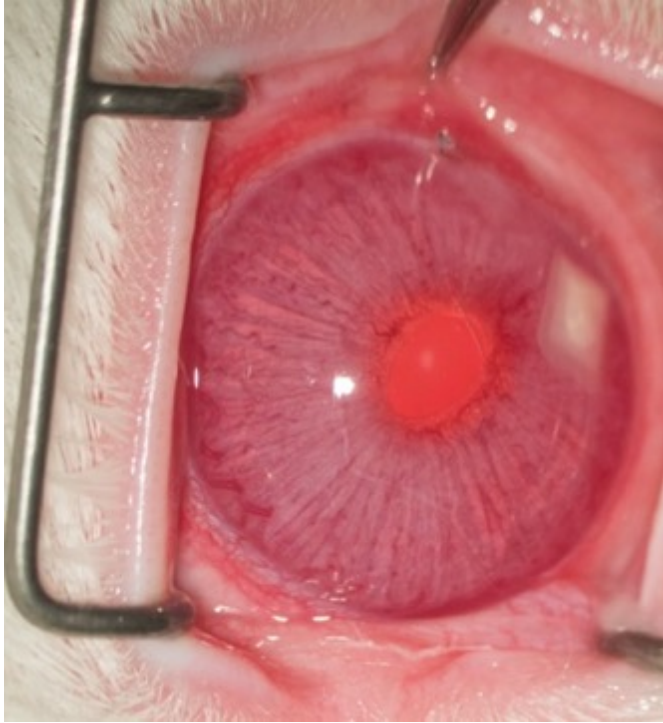


Figure 3.1 Representative ocular photo after device implantation in the anterior chamber taken before euthanasia.

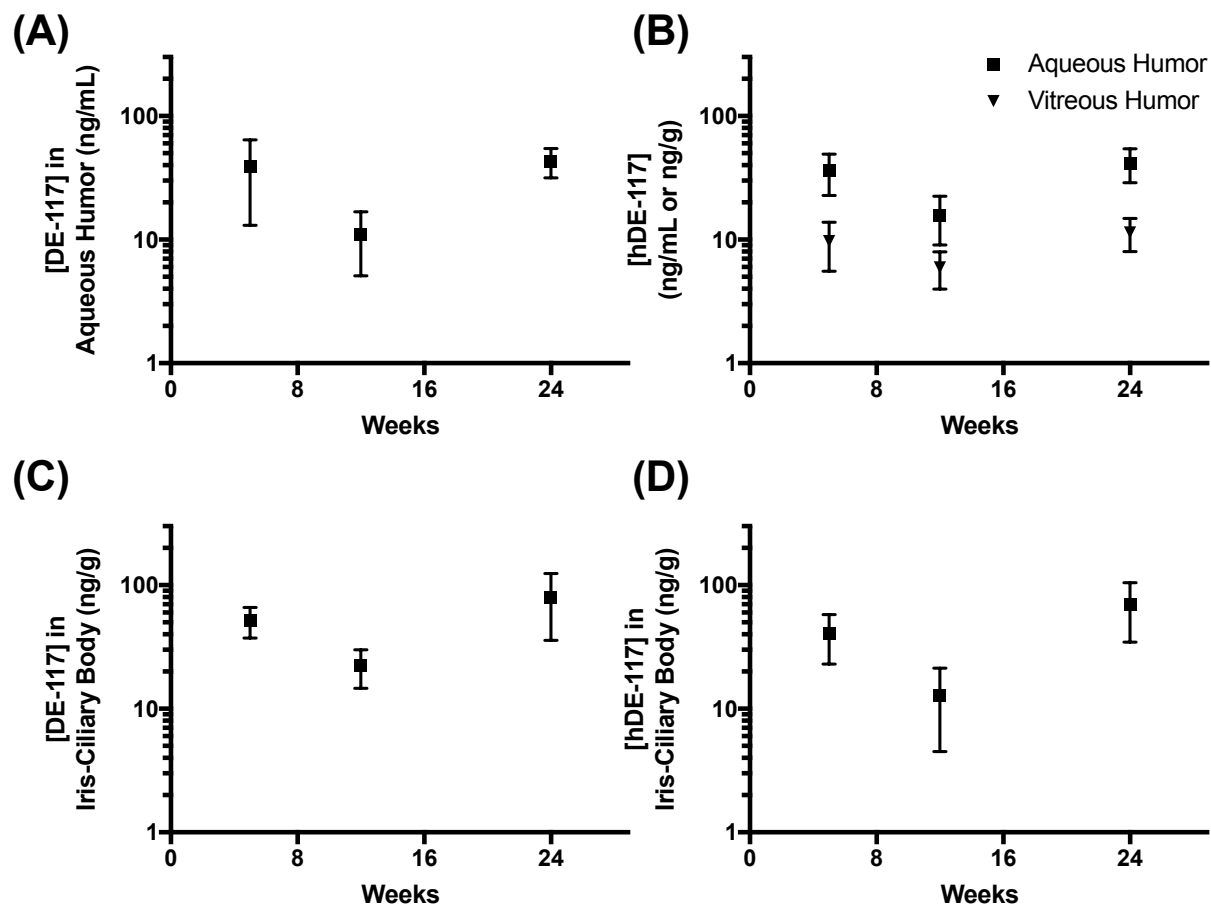


Figure 3.2 Concentration of DE-117 and hDE-117 in the aqueous humor and vitreous (A,B) and iris-ciliary body (C,D) 5, 12, and 24 weeks after DE-117-loaded device implantation. Concentration of DE-117 in the vitreous was below the limit of quantification.

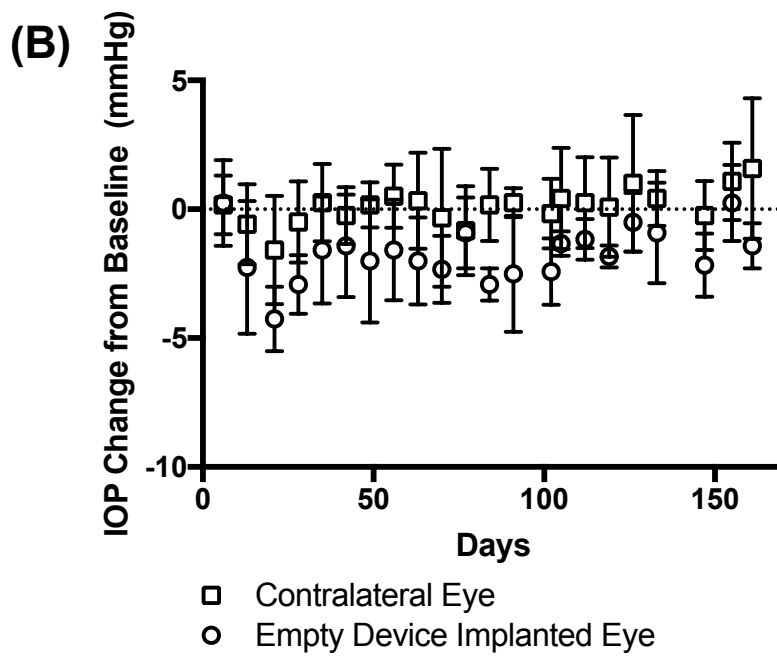
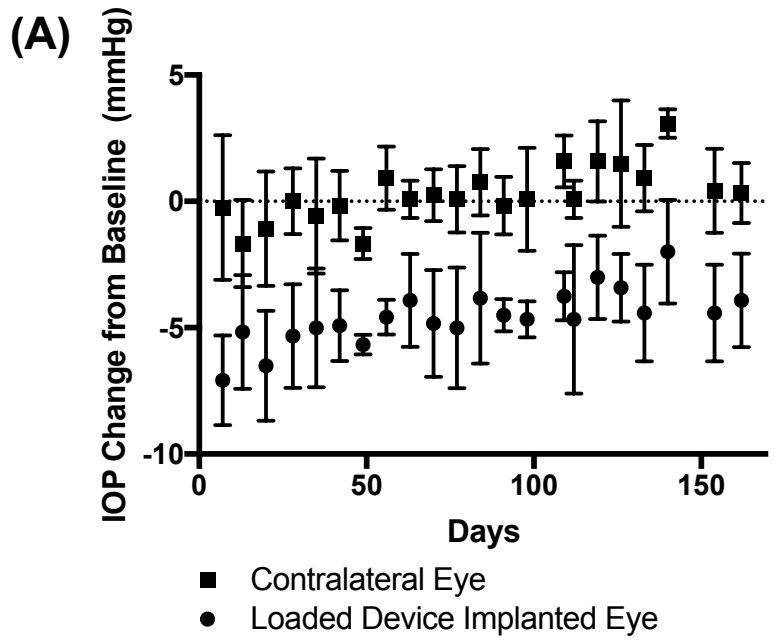


Figure 3.3 IOP change from baseline for eyes with **(A)** DE-117 loaded or **(B)** empty device implantation compared to their contralateral (untreated) eyes. Data is shown as mean \pm standard deviation.

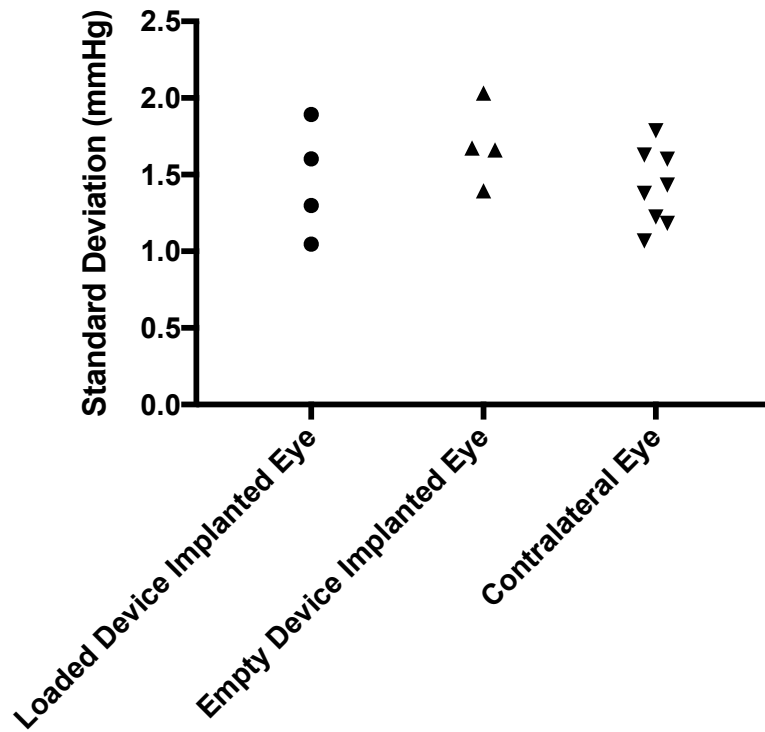


Figure 3.4 Long-term IOP fluctuation, defined as the standard deviation of IOP measurements at all time points, among different treatment groups.

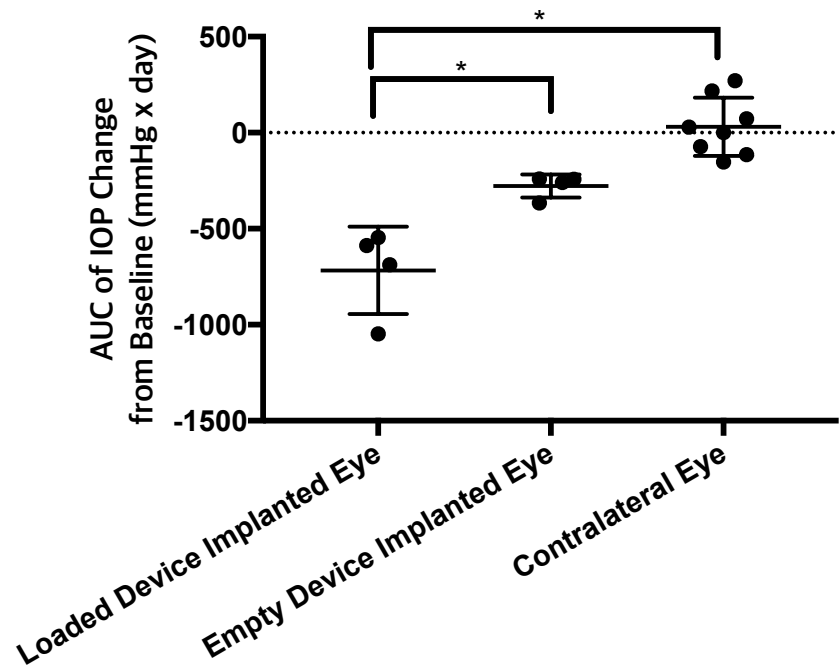


Figure 3.5 Cumulative IOP reduction represented by the AUC of IOP change from baseline. Reduction in IOP from baseline was calculated as negative area. Data is shown as mean \pm standard deviation.

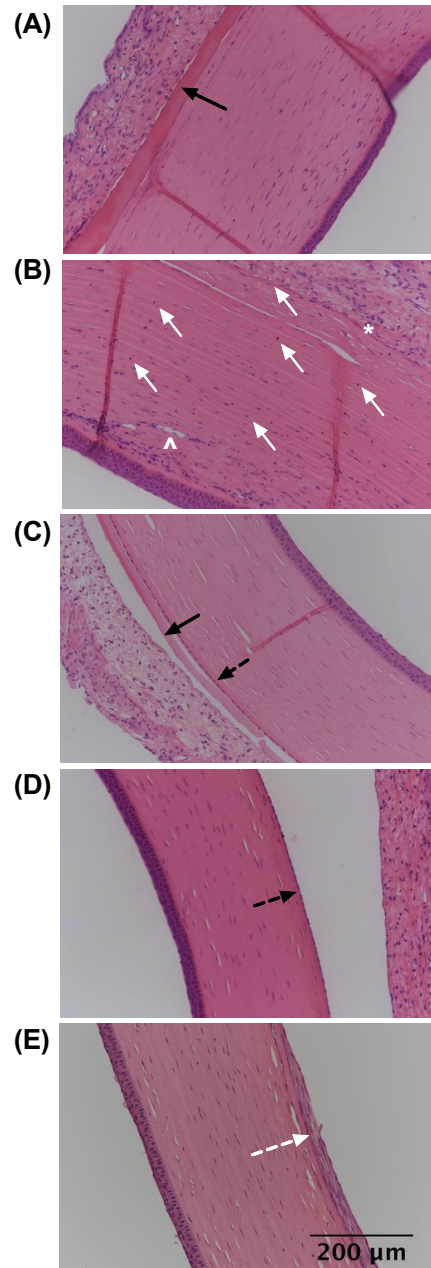


Figure 3.6 Histological images of the rabbit cornea (**A,B,C,E**) after 24 weeks of device (without drug) implantation and (**D**) without implantation (contralateral eyes). Eye shown in (**A,B**) (n=1) exhibited partial corneal opacification and neovascularization, which was not observed in other eyes (n=7) (**C,D,E**). Black arrow = accumulation of eosinophilic exudate, white arrow = inflammatory cells and corneal endothelial attenuation, black dotted arrow = corneal

endothelium, white asterick = anterior synechia, white arrowhead = stromal neovascularization,
and white dotted arrow = corneal endothelial metaplasia.

Chapter 4 – Co-delivery of hypotensive agents using PCL implants

4.1 Abstract

Glaucoma is a major leading cause of irreversible blindness worldwide. While glaucoma is typically treated by pressure-lowering eye drops, the high frequency of administration (up to 3 times daily) is a persisting challenge to patient compliance and efficacious treatment. Here, we developed an intracameral ocular implant that can deliver two glaucoma drugs with controlled release kinetics using diffusion-limiting polymer films. The drug delivery implant designed to last up to 3 months will be less dependent on patient compliance compared to the conventional eye drop. Furthermore, an implant that releases more than one therapeutic can enable efficacious treatment of glaucoma patients who do not respond to monotherapy.

4.2 Introduction

In addition to the barriers to glaucoma treatment mentioned earlier, many patients require combination therapy utilizing more than one hypotensive agent is required for sufficient IOP control. For example, studies showed that roughly half of glaucoma patients do not achieve sufficient IOP reduction with monotherapy [61]. As an example of combination therapy for glaucoma, previous studies showed that co-administration of timolol maleate and brimonidine tartrate has superior IOP reducing effects in glaucoma patients compared to those receiving monotherapy [62, 63]. Considering the burden of patient compliance associated with dosing additional hypotensive agents, fixed combination eye drops were introduced; specifics of various fixed combination glaucoma therapies are thoroughly described in several reviews [61, 64, 65]. In short, many hypotensive agents are available in the form of fixed dose combination, including

β -blockers, adrenergic agonists, prostaglandin analogs, and carbonic anhydrase inhibitors [66]. While fixed combination medications allow more convenient mode of therapy for glaucoma patients that require more than one hypotensive agent, it still requires patient compliance in the form of eye drops at least daily. In other words, the challenge of patient compliance also affects glaucoma patients who do not sufficiently respond to monotherapy.

To address this issue, we developed a two-compartment intracameral implant using PCL thin films as diffusion-limiting barriers. The device encapsulates pellets of two glaucoma medications (timolol maleate and brimonidine tartrate) in separate compartments. By changing the thickness of the diffusion-limiting thin film, release rates of two drugs are tuned to meet their desired concentration in the front of the eye. The device can be loaded with enough drug to last 6 months of release and has the potential to achieve additive IOP drop during drug release.

4.3 Materials and methods

4.3.1 Materials

All chemicals were obtained from Sigma-Aldrich Corporation (St. Louis, MO, USA) unless noted otherwise. Timolol maleate was obtained from Sigma-Aldrich and brimonidine tartrate was obtained from Cayman Chemical (Ann Arbor, MI, USA).

4.3.2 Co-delivery device fabrication

To encapsulate glaucoma drugs in separate compartments, two PCL films were stacked and sealed by selectively heating the edges. Drugs were loaded in powder form. PCL thin films were made by spin-casting a solution of PCL in 2,2,2-trifluoroethanol (TFE) at a concentration of 150 mg/mL. The desired thickness was achieved by changing total time of spin. Spun-cast PCL films were left to dry in the fume hood, heated to 110 °C, and cooled to room temperature to remove residual solvent. Film thickness was measured using a micrometer (iGaging, San Clemente, CA, USA). Target release rate was optimized based on the potency of each glaucoma drug (timolol maleate and brimonidine tartrate) and was achieved by adjusting the thickness of the PCL film. Compartment containing timolol maleate was made using films with thickness of 45 µm and compartment loaded with brimonidine tartrate was made using 23 µm-thick films. Each compartment was fabricated separately and sealed together at one edge to create a single device that can be implanted in the anterior chamber.

4.3.3. In vitro drug release analysis

Drug release from each drug-containing compartment was tested by submerging in 0.5 mL of phosphate buffered saline (PBS) at 37 °C. PBS was used because the aqueous humor, which fills the anterior chamber and serves as the release medium in the eye, mostly consists of water and has near neutral pH [67]. Release medium was replaced with fresh PBS at each time point. Concentration of drug was quantified by UV-Vis spectrometry at absorption wavelengths of timolol = 294 nm and brimonidine = 254 nm. After drug release from each compartment was characterized, devices that show signs of defect, which was likely introduced during the heat-sealing process, were eliminated. Following quality control of devices, the two devices were

sealed together and underwent consequent drug release study to confirm that the final sealing step did not affect device integrity.

4.4 Results and discussion

We developed a drug delivery implant, smaller than a grain of rice, that can deliver two glaucoma drugs as shown in Figure 4.1. The implant contains two compartments, each containing timolol or brimonidine, that are stacked together to create a single device. We show that our co-delivery glaucoma implants achieve controlled release of two glaucoma drugs (timolol: 5.2 $\mu\text{g}/\text{day}$ and brimonidine: 0.56 $\mu\text{g}/\text{day}$) currently used in the clinic (Figure 4.2). Assuming a 30 μL eye drop volume, topical dosage can be approximately 300 $\mu\text{g}/\text{day}$ for timolol (0.5% w/v, 2 drops/day) and 90 $\mu\text{g}/\text{day}$ for brimonidine (0.1% w/v, 3 drops/day). Since ocular bioavailability upon topical administration is typically less than 5% [5], our drug delivery implants have the potential to reach therapeutically meaningful concentration of both drugs in the eye.

Future work includes in vivo pharmacokinetic analysis by implanting the co-delivery devices in the intracameral space of rabbit eyes. After optimization of release rates based on the pharmacokinetic analysis, IOP-reducing efficacy of co-delivery should be assessed in another animal model considering previous reports that showed only slight IOP reduction in normotensive rabbits with topical timolol administration [68]. Another study reported that timolol reduces IOP in normotensive rabbits only when applied in the dark phase of the circadian cycle [69]. Dogs may be a good model for the efficacy analysis since topical

administration of timolol solution [70] or timolol maleate gel-forming solution [71] have been shown to significantly reduce IOP. Furthermore, the compatibility of the device design with other drug combinations should be explored considering the wide range of fixed dose combinations that have been explored in the clinic.

4.5 Conclusion

We demonstrated proof-of-concept fabrication of drug delivery devices that can achieve release of two glaucoma agents in vitro. Based on preliminary evaluation of devices' release kinetics, we showed that drug release rates are within desirable range. Future works include long-term in vitro release studies and pharmacokinetic evaluation in rabbits. If successful, our drug delivery implant can enable more effective therapy for many glaucoma patients suffering from the burden of frequent drug administration.

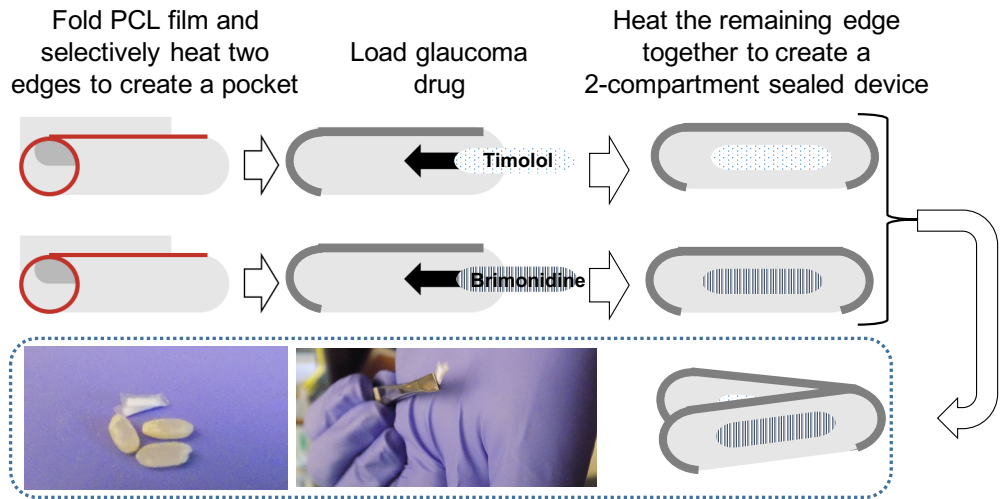


Figure 4.1 Schematic diagram of drug delivery device fabrication for co-delivery of glaucoma agents. The resulting co-delivery device is smaller than a grain of rice.

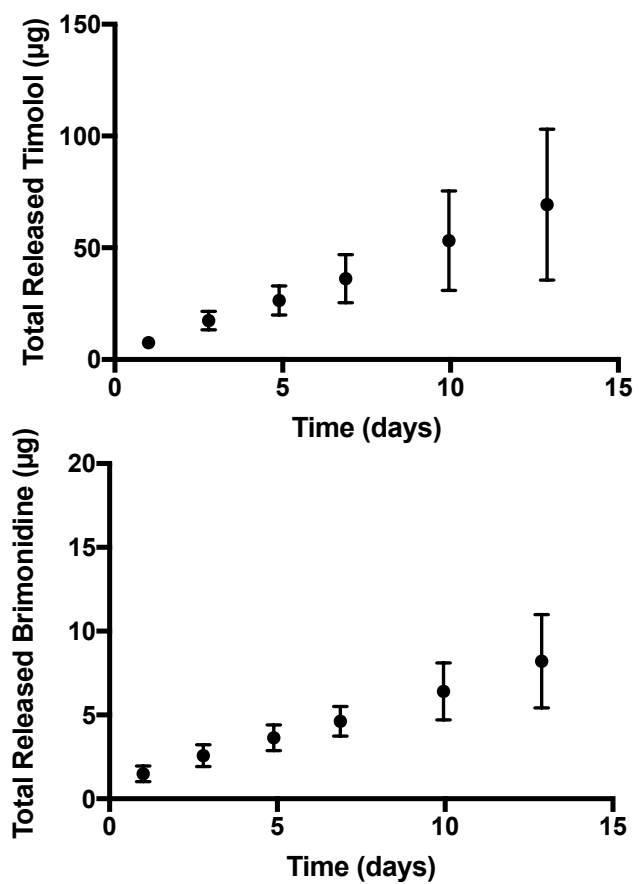


Figure 4.2 In vitro release rates of timolol maleate and brimonidine tartrate from individual compartments of the co-delivery device.

Chapter 5 – PCL blending for intracameral drug delivery application

5.1 Abstract

Polycaprolactone (PCL) has been widely used in biomedical research applications thanks to its biodegradability and biocompatibility. While time to PCL fragmentation can be tuned by reducing its starting molecular weight, thin films made from low molecular weight PCL are limited in its compatibility with fabrication techniques utilized to make aforementioned drug delivery devices. To overcome this limitation, blends of low, medium, high molecular weight PCL were investigated to achieve lower starting molecular weight of PCL without adversely affecting the film's mechanical properties. Both number- and weight-average molecular weights of various blends were calculated to identify the representative parameter that estimates film fragmentation properties. Also, tensile strength testing was performed to assess the mechanical properties of blended films compared to unblended films. Based on qualitative analysis of the films produced from blended PCL solutions, we identified the weight-average molecular weight to be the representative parameter in fragmentation behavior. Also, evaluation of mechanical properties showed that low molecular weight PCL can be blended with high molecular weight PCL with mass ratio of 3:1 without substantially affecting the ultimate tensile strength of resulting film. In summary, PCL blending shows promise as a method to achieve versatile control of PCL film degradation without limiting the manufacturing capabilities of PCL drug delivery devices.

5.2 Introduction

Polycaprolactone (PCL), a biodegradable polyester, has been widely used in biomedical research applications, including drug delivery [40-44, 53], tissue engineering [72-74], and medical devices such as stents [75-77]. Numerous studies reported positive biocompatibility of PCL in vitro [78, 79] and in vivo, including the ocular space [45]. Previous studies demonstrated that PCL degrades primarily via bulk degradation through hydrolytic random chain scission [50]. Based on the autocatalytic degradation model proposed by Pitt et al, time to PCL fragmentation is dependent on the starting molecular weight and rate of degradation, as shown in the equation below [50].

$$M_n = M_n^0 \times e^{-k't}$$

where M_n is the number-averaged molecular weight after a certain length of time (t), M_n^0 is the starting number-averaged molecular weight, and k' is the rate constant. Based on this model and previously published k' value, PCL with approximately $M_n = 80,000$ Da, which was used in our ocular drug delivery studies presented in earlier chapters, would take approximately 2.8 years to reach fragmentation point (approximately $M_n = 5,000$ Da [50] or $M_w = 8,000$ Da [51]). While a glaucoma implant that lasts several years may have some benefits, the ability to tune PCL's time to fragmentation will allow more versatile application of PCL drug delivery systems that require complete device degradation in a shorter period of time. For example, a drug delivery implant that requires a high drug release rate will require a larger initial payload for extended release and/or more frequent device implantation. The ability to make devices that degrade in a shorter period of time will help prevent unnecessary accumulation of void devices in the eye.

Since time to PCL fragmentation is dependent on the starting molecular weight as shown in the equation above, one can use a lower starting molecular weight to achieve shorter time to fragmentation. While PCL with lower molecular weights is available, thin films made from lower molecular weight PCL tend to be fragile and incompatible with the device fabrication process previously described. To address this challenge, we explored a blending approach involving PCL with high ($M_n = 80$ kDa), medium ($M_n = 45$ kDa), and low ($M_n = 10$ kDa) molecular weights. By blending, PCL thin film with lower starting molecular weight may be achieved without substantially affecting the mechanical properties of the film. The number- (M_n) and weight-averaged (M_w) molecular weights of blends can be calculated using the equations shown below [81].

$$M_n = \frac{1}{\sum_i \frac{w_i}{M_{n,i}}}$$

$$M_w = \sum_i w_i M_{w,i}$$

w_i = mass fraction of polymer (i) with $M_{n,i}$ and $M_{w,i}$

In addition, various polymer blending approaches have been widely studied to enhance the mechanical properties of the unblended polymer. Examples include blending PCL with chitosan [82], wheat thermoplastic starch (TPS) [83], polylactide (PLA) [84], and many others. The effects of mixing high and low molecular weight polymers have been investigated in several applications [85-87] including those focused on drug release characteristics [86, 87]. However, the mechanical properties of blended PCL films for drug delivery applications have not been extensively studied.

In this study, we investigated the molecular weight distribution of a range of blends consisting of high, medium, and low molecular weight PCL. In addition, based on the starting molecular weight calculation, we tentatively identified a parameter that may be used to estimate the time to fragmentation of blends. Furthermore, we performed tensile strength testing on unblended and blended PCL thin films to evaluate the effect of blending on their mechanical properties, such as ultimate tensile strength, elastic modulus, and elongation to break.

5.3 Materials and methods

5.3.1 Materials

All materials were obtained from Sigma-Aldrich Corporation (St. Louis, MO, USA) unless noted otherwise.

5.3.2 PCL film fabrication and characterization

A solution of PCL was casted using a multiple clearance square applicator (Paul N. Gardner Company, Inc., Pompano Beach, FL, USA) at a concentration of 150 mg/mL dissolved in 2,2,2-trifluoroethanol. Various PCL blends were made by changing the mass ratio of high, medium, and low molecular weight PCL while keeping the total polymer concentration constant at 150 mg/mL. The casted PCL films were dried in the fume hood, heated to remove residual solvent,

and left to dry at room temperature. Thickness of the casted films were measured using a film micrometer (iGaging, San Clemente, CA, USA).

5.3.3 Gel permeation chromatography (GPC) analysis

PCL molecular weight distributions were determined via GPC (1260 Infinity Quaternary LC System, Agilent Technologies, Santa Clara, CA). An isocratic method with tetrahydrofuran (THF) (VWR, Radnor, PA, USA) as the running buffer was used with a series of a guard column (WAT054405; Waters Corporation, Milford, MA, USA) and four Styragel® GPC columns (HR5/WAT0554460, HR4/WAT044225, HR2/WAT044234, HR0.5/WAT044231; Waters Corporation) and a refractive index detector (RID). A flow rate of 1 mL/min was used for 50 minutes. Molecular weight analysis was completed using a universal calibration method based on polystyrene standards. Two sets of polystyrene standards (low molecular ReadyCal (M_p 250 - 70,000) and ReadyCal (M_p 400 - 2,000,000)) were analyzed via GPC with triple technical replicates. The average peak retention time of technical replicates was used to create a linear standard curve of $\log(M_p)$ versus retention time (Figure 5.1). The standard curve was used to convert the x-axis of raw RID signal from retention time to molecular weight of polymer chains. To account for differences in polymer type (polystyrene standards and PCL test samples), the x-axis was adjusted using literature-reported Mark-Houwink coefficients for polystyrene and PCL [88]. RID signal with a blank solvent (THF) sample was subtracted from the raw sample RID signal to account for the signal from the solvent. Signal below baseline (negative signal) was considered noise and converted to baseline (0).

5.3.4 Tensile testing

Tensile testing was performed by Westpak, Inc. (San Jose, CA, USA) based on the general guidelines of ASTM D882-12: Tensile Properties of Thin Plastic Sheeting using a Shimadzu load frame (AG-I/50N – 10kN) and a 1 kN load cell (SLBL-1kN) (Kyoto, Japan). PCL films were cut in 1 by 3 inch strips before testing. All films (n=3 per condition) were measured with a jaw separation rate of 13 mm/min, except films 1 and 2 that used a rate of 508 mm/min. Ultimate tensile strength was defined as the maximum force reached before film failure. Modulus of elasticity was approximated from the force versus displacement curve. Elongation to break was defined as the elongation reached immediately before film failure or at the end of test cycle.

5.4 Results

5.4.1 Starting molecular weights of PCL blends

Starting molecular weights of unblended PCL were compared with those provided by the vendor as shown in Table 5.1. While there is some variability, the experimentally calculated M_n and M_w values appear to be in line with the values provided by the vendor. Using the experimentally calculated M_n and M_w from the GPC analysis, M_n and M_w of blends were calculated (Table 5.2). As the blends were made by mixing PCL with different mass ratios, M_n of blends were generally lower than their M_w . For example, PCL blend of 1:1 (mass ratio) 80 kDa:10 kDa (assuming M_w values of 140 kDa and 17 kDa respectively) resulted in $M_w = 79$ kDa and $M_n = 18$ kDa. Films made from $M_n = 10$ kDa PCL alone fragmented upon casting and could not be removed intact

from the casted surface. If M_n was the representative parameter in estimating the molecular weight at fragmentation for blends, a blend film with $M_n = 17$ kDa would be expected to exhibit similar fragmentation behaviors as an unblended film with $M_n = 10$ kDa. However, in terms of ease of handling, films made from PCL blend of 1:1 80 kDa:10 kDa showed more similarity to unblended 80 kDa film. The general trend applied to the rest of blended films assessed as well (Table 5.2). Based on the qualitative evaluation of the ability to handle thin film with comparable thicknesses, M_w appears to be the relevant parameter in the assessment of thin films in their device fabrication potential.

5.4.2 Molecular weight distribution of blends

Molecular weight distribution of polymer chains, characterized by GPC analysis, is shown in Figure 5.2. Figure 5.2.A shows molecular weight distribution of unblended PCL with low, medium, and high molecular weights. The peak retention time of blended PCL appears to be in close proximity to those of unblended PCL components (Figure 5.2).

5.4.3 Mechanical properties of blended films

Ultimate tensile strength, elastic modulus, and elongation at break of unblended and blended thin film strips of PCL were analyzed via tensile strength testing (Figure 5.3). Comparing blends of 80 kDa and 10 kDa PCL only, ultimate tensile strength of thin films was not noticeably affected up to 75% (mass ratio) of 10 kDa blending. Elastic modulus of thin films showed a general increasing trend with more low molecular weight PCL blended. As expected, elongation at break

showed that the films were less able to stretch when more low molecular weight PCL is blended, likely due to the shorter polymer chain's limited ability to stretch compared to that of longer polymer chains.

5.5 Discussion

As part of a systematic investigation of various PCL blends covering a range of M_n and M_w (shown in Table 5.2), qualitative assessment of the films was performed after casting. For example, films that were made with 90% or 100% 10 kDa PCL exhibited fragmentation behaviors immediately upon casting and could not be removed from the casting surface in one piece. This evaluation allowed comparison of M_n and M_w regarding its relevancy in estimating point of film fragmentation. For example, if M_n represented fragmentation time, blends with similar starting M_n values would be expected to show similar fragmentation behaviors. However, while blend 11 could be handled for mechanical testing, blend 13 and film 14 showed signs of fragmentation upon casting despite the small difference in their M_n . From these assessments, M_w was determined to be the more relevant parameter in determination of fragmentation limits. This is an interesting observation as many literature reports primarily use M_n as the parameter of interest in evaluating PCL degradation [50].

To assess our general observation that films made from blends are less fragile than unblended films, ultimate tensile strength (tensile strength at break) of various blends were compared (Figure 5.3). Ultimate tensile strength of 80 kDa PCL film (17.1 ± 0.9 MPa) was similar to what has been reported in literature (ranging from 10.5 to 16.1 MPa for bulk PCL with $M_n = 91,900 \pm$

7,700 Da [89]). Interestingly, ultimate tensile strength of unblended 80 kDa PCL film was similar to that of films 2, 5, 7, and 9, which contained 33%, 50%, 67%, and 75% (w/w) 10 kDa PCL respectively. However, once 83% 10 kDa PCL was blended (film 11), ultimate tensile strength of the resulting film was substantially reduced. This result indicated that tensile strength of PCL can remain unaffected with 10kDa PCL blending until a certain blending percentage (75%).

Furthermore, PCL blends can be used to produce films that are better compatible with device fabrication than unblended PCL. With respect to this approach for tuning PCL degradation, it is important to understand how differences in PCL molecular weight distribution impact film permeability. Our preliminary results indicate that small molecule (atenolol and timolol) permeation through blended films are not affected compared to that through unblended films. We noted that in a previous report on blending high and low molecular weight PLA, a change in diffusive drug release was observed upon blending [87]. However, while their study utilized direct mixing of model drug in the polymer solution for casting or emulsification, our study focused on using PCL blends for fabrication of thin film devices encapsulating a pellet of drug. In these encapsulation devices, diffusion of drug through the film is unlikely to change by blending, unless blending introduces imperfections to the film, such as pores, that affect the film's role as a diffusive barrier. As blending does not appear to impact permeability of small molecules through PCL films, our results suggest that blending can be used to fabricate drug delivery devices without change in drug release kinetics. However, more thorough permeability testing involving drugs with a range of properties should be performed to confirm this conclusion.

5.6 Conclusion

Blends of low and high molecular weight PCL showed promise in reducing average starting molecular weight without substantially affecting the mechanical properties of the resulting thin films. Future studies will investigate the degradation kinetics of the blended films in a physiologically relevant condition in vitro as well as in the ocular space in an animal model. Furthermore, drug release kinetics from drug delivery devices made from PCL blends will be more thoroughly analyzed by testing various drugs covering a range of drug properties, such as molecular weight and solubility.

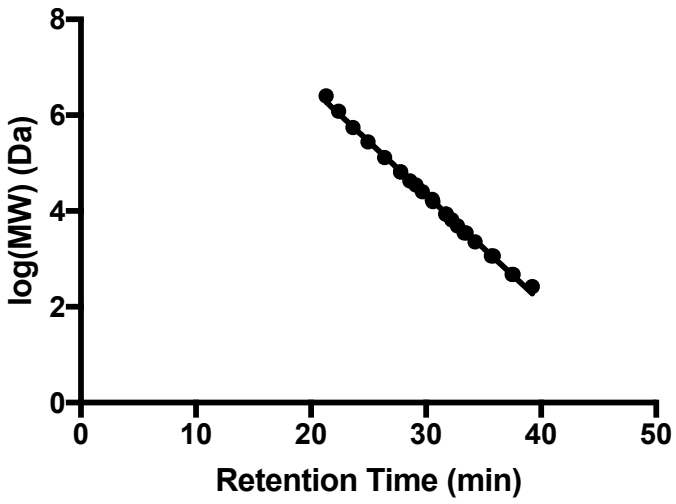


Figure 5.1 Relationship between polystyrene standards' molecular weight and peak retention time during GPC analysis used to convert the retention time to molecular weight.

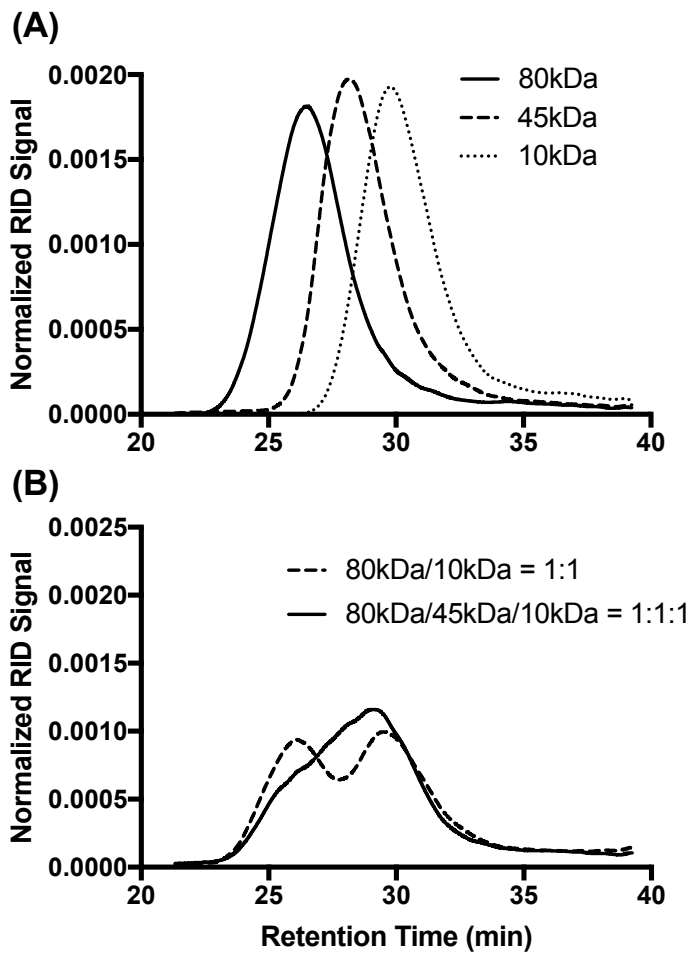


Figure 5.2 Molecular weight distribution of **(A)** unblended and **(B)** selected blended PCL.

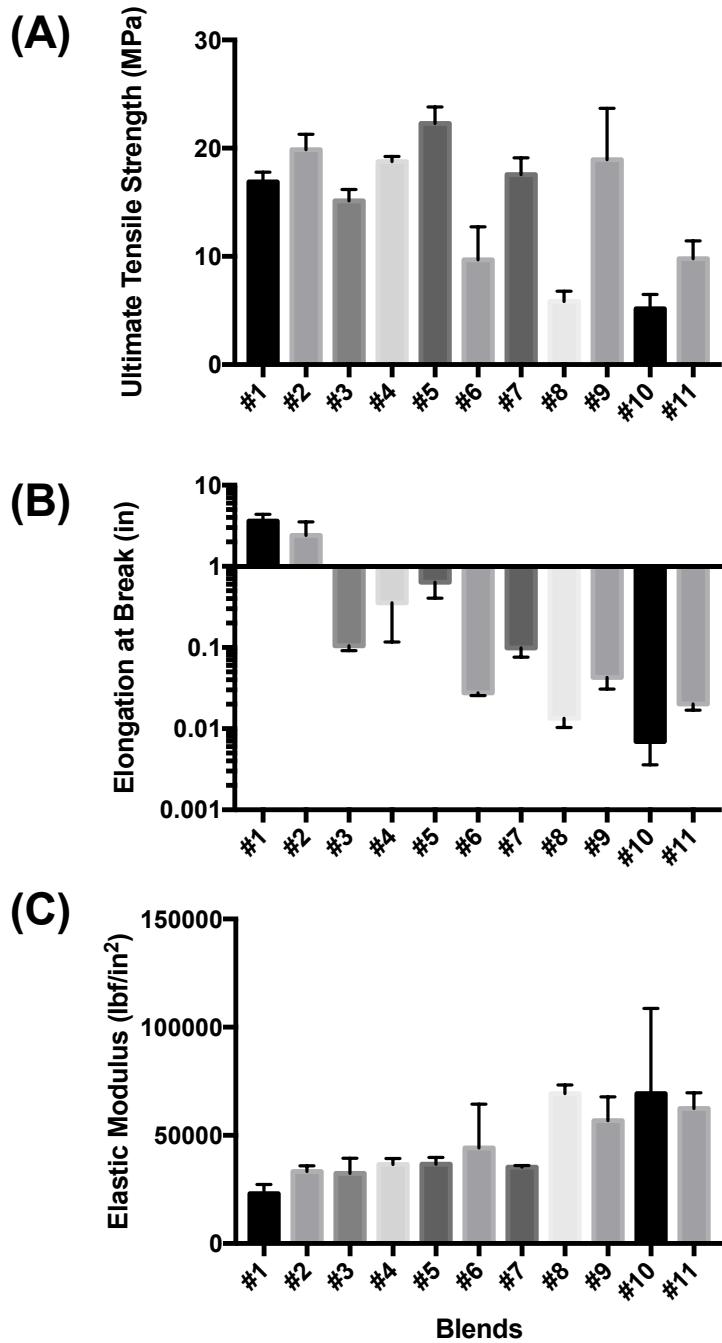


Figure 5.3 Evaluation of mechanical properties of unblended and blended PCL via tensile strength testing, showing (A) ultimate tensile strength, (B) elongation at break, and (C) elastic modulus. Film numbers corresponds to different blending ratios shown in Table 5.2.

Table 5.1 Average molecular weights of unblended PCL comparing vendor-provided values and experimentally calculated values.

Molecular weight	Vendor provided		Experimentally calculated	
	M_n (kDa)	M_w (kDa)	M_n (kDa)	M_w (kDa)
Low	~10	~14	14	22
Medium	45 (40 – 50)	(48 – 90)	30	50
High	80	N/A	84	140

Table 5.2 Mass ratios of PCL blending among low (10 kDa), medium (45 kDa), and high (80 kDa) PCL and the resulting M_n and M_w . M_n and M_w of PCL was calculated using the experimentally calculated M_n and M_w values of unblended PCL.

	Mass Fraction			M_n (kDa)	M_w (kDa)
	Low	Medium	High		
1			1.00	84	140
2	0.33		0.67	32	101
3		1.00		30	50
4	0.33	0.33	0.33	26	70
5	0.50		0.50	24	81
6	0.33	0.67		22	41
7	0.67		0.33	19	61
8	0.50	0.50		19	36
9	0.75		0.25	18	52
10	0.67	0.33		17	31
11	0.83		0.17	16	42
12	0.80	0.20		16	28
13	0.90		0.10	15	34
14	1.00			14	22

Chapter 6 Summary and conclusions

Treatment of glaucoma, a major leading cause of irreversible blindness worldwide, is limited due to the great burden of compliance imposed on the patients as well as the ocular physiological barriers that result in very low bioavailability of glaucoma drugs. Considering the potentially dire consequences of patient non-compliance in glaucoma and the chronic nature of the disease, polycaprolactone (PCL) thin film devices, which can deliver one or more hypotensive agents with controlled release kinetics directly to the anterior chamber, have substantial potential to improve therapeutic outcome for glaucoma patients.

First, PCL thin film intracameral implants containing a proprietary hypotensive agent were developed, characterized, and evaluated *in vitro* and *in vivo* for the treatment of glaucoma. The studies showed that PCL thin film drug delivery devices are able to achieve long-term controlled drug release *in vitro* as well as sustained drug distribution in ocular tissues and reduction in intraocular pressure (IOP) *in vivo*.

The potential of PCL thin film devices for glaucoma combination therapy have also been evaluated by the development of two-compartment drug delivery devices containing timolol maleate and brimonidine tartrate, which are hypotensive agents currently used in the clinic. The studies showed that by tuning film thickness, PCL thin film devices are able to provide controlled release of each therapeutic with specifically tuned release rates.

Lastly, a polymer blending approach was investigated in order to tune the PCL film's time to fragmentation without negatively affecting the film's compatibility with device manufacturing methods. By blending low and high molecular weight PCL, PCL thin film with lower starting

molecular weight could be made without substantially affecting its mechanical properties, such as its ultimate tensile strength.

Future studies should be focused on developing a more controlled manufacturing method for the thin film devices to achieve miniaturization of device size. Also, the pharmacokinetic and efficacy evaluations should be performed in larger animals that better mimic the physiological conditions in humans. Furthermore, degradation kinetics of PCL blends should be evaluated in vitro and in vivo to confirm that blends with lower starting molecular weights achieve shorter time to fragmentation in the eye as expected. With further optimization and characterization, PCL thin film devices show great promise as a mode of long-term glaucoma therapy.

References

1. Tham YC, Li X, Wong TY, Quigley HA, Aung T, Cheng CY. Global prevalence of glaucoma and projections of glaucoma burden through 2040: A systematic review and meta-analysis. *Ophthalmology*. 2014;121(11):2081-2090. doi:10.1016/j.ophtha.2014.05.013.
2. Allingham RR, Shields MB. *Shields' textbook of glaucoma*. Philadelphia, PA: Lippincott Williams & Wilkins;2005.
3. Heijl A, Leske C, Bengtsson B, Hyman L, Bengtsson B, Hussein M. Reduction of intraocular pressure and glaucoma progression. *Arch Ophthalmol*. 2002;120:1268-1279.
4. Leske CM, Heijl A, Hussein M, Bengtsson B, Hyman L, Komaroff E. Factors for glaucoma progression and the effect of treatment. *Arch Ophthalmol*. 2003;121:48-56.
5. Urtti A. Challenges and obstacles of ocular pharmacokinetics and drug delivery. *Adv Drug Deliv Rev*. 2006;58(11):1131-1135. doi:10.1016/j.addr.2006.07.027.
6. Deng F, Ranta V-P, Kidron H, Urtti A. General pharmacokinetic model for topically administered ocular drug dosage forms. *Pharm Res*. 2016;56. doi:10.1007/s11095-016-1993-2.
7. Occhipinti JR, Mosier MA, LaMotte J, Monji GT. Fluorophotometric measurement of human tear turnover rate. *Curr Eye Res*. 1988;7(April):995-1000. doi:10.3109/02713688809015145.
8. Urtti A. Delivery of antiglaucoma drugs: ocular vs systemic absorption. *J Ocul Pharmacol*. 1994;10(1):349-357. <http://www.ncbi.nlm.nih.gov/pubmed/8207339>.

9. Cox A. Systemic effects of ocular drugs. *Adverse Drug Reaction Bulletin*. London, UK: Lippincott Williams & Wilkins;2002.
10. Kaila T, Salminen L, Huupponen R. Systemic absorption of topically applied ocular timolol. *J Ocul Pharmacol*. 1985;1(1):79-83.
11. The Friedenwald Lecture. Flow of aqueous humor in humans. *Invest Ophthalmol Vis Sci*. 1991;32(13):3145-3166.
12. Fontana ST, Brubaker RF. Volume and depth of the anterior chamber in the normal aging human eye. *Arch Ophthalmol*. 1980;98(10):1803-1808.
<http://www.ncbi.nlm.nih.gov/pubmed/7425907>.
13. Kholdebarin R, Campbell RJ, Jin Y-P, Buys YM. Multicenter study of compliance and drop administration in glaucoma. *Can J Ophthalmol*. 2008;43(4):454-461.
doi:10.3129/I08-076.
14. Gordon M, Beiser J, Brandt JD, et al. The ocular hypertension treatment study: Baseline factors that predict the onset of primary open-angle glaucoma. *Arch Ophthalmol*. 2002;120:714-720. doi:10.1001/archophthalmol.2008.599.
15. Burns E, Mulley GP. Practical problems with eye-drops among elderly ophthalmology outpatients. *Age Ageing*. 1992;21(3):168-170.
16. Taylor SA, Galbraith SM, Mills RP. Causes of non-compliance with drug regimens in glaucoma patients: a qualitative study. *J Ocul Pharmacol Ther*. 2002;18(5):401-409.
doi:10.1089/10807680260362687.
17. Gurwitz JH, Glynn RJ, Monane M, et al. Treatment for glaucoma: Adherence by the elderly. *Am J Public Health*. 1993;83(5):711-716. doi:10.2105/AJPH.83.5.711.

18. Lisboa R, Chun YS, Zangwill LM, et al. Relationship between rates of binocular visual field loss and vision-related quality of life in glaucoma. *JAMA Ophthalmol*. 2013;131(4):486-494. doi:10.1001/jamaophthalmol.2013.2602.
19. van Gestel A, Webers CAB, Beckers HJM, et al. The relationship between visual field loss in glaucoma and health-related quality-of-life. *Eye (Lond)*. 2010;24(12):1759-1769. doi:10.1038/eye.2010.133.
20. American Foundation for the Blind. Key Findings: National Poll on Severe Vision Loss/Blindness website. <http://www.afb.org/info/programs-and-services/public-policy-center/policy-research/national-poll-findings-3376/1235>. 2007. Accessed June 5, 2016.
21. Carvalho IM, Marques CS, Oliveira RS, Coelho PB, Costa PC, Ferreira DC. Sustained drug release by contact lenses for glaucoma treatment - A review. *J Control Release*. 2015;202:76-82. doi:10.1016/j.jconrel.2015.01.023.
22. Ali M, Horikawa S, Venkatesh S, Saha J, Hong JW, Byrne ME. Zero-order therapeutic release from imprinted hydrogel contact lenses within in vitro physiological ocular tear flow. *J Control Release*. 2007;124(3):154-162. doi:10.1016/j.jconrel.2007.09.006.
23. Maulvi FA, Lakdawala DH, Shaikh AA, et al. In vitro and in vivo evaluation of novel implantation technology in hydrogel contact lenses for controlled drug delivery. *J Control Release*. 2016;226:47-56. doi:10.1016/j.jconrel.2016.02.012.
24. Ciolino JB, Hoare TR, Iwata NG, et al. A drug-eluting contact lens. *Investig Ophthalmol Vis Sci*. 2009;50(7):3346-3352. doi:10.1167/iovs.08-2826.

25. Ciolino JB, Ross AE, Tulsan R, et al. Latanoprost-eluting contact lenses in glaucomatous monkeys. *Ophthalmology*. 2016;123(10):2085-2092. doi:10.1016/j.ophtha.2016.06.038.
26. Park CG, Kim YK, Kim MJ, et al. Mucoadhesive microparticles with a nanostructured surface for enhanced bioavailability of glaucoma drug. *J Control Release*. 2015;220:180-188. doi:10.1016/j.jconrel.2015.10.027.
27. Choy YB, Park J-H, McCarey BE, Edelhauser HF, Prausnitz MR. Mucoadhesive microdiscs engineered for ophthalmic drug delivery: Effect of particle geometry and formulation on preocular residence time. *Investig Ophthalmol Vis Sci*. 2010;9(2):1-14. doi:10.1111/j.1600-6143.2008.02497.x.Plasma.
28. Park CG, Kim MJ, Park M, et al. Nanostructured mucoadhesive microparticles for enhanced preocular retention. *Acta Biomater*. 2014;10(1):77-86. doi:10.1016/j.actbio.2013.08.026.
29. Jiang J, Gill HS, Ghate D, et al. Coated microneedles for drug delivery to the eye. *Investig Ophthalmol Vis Sci*. 2007;48(9):4038-4043. doi:10.1167/iovs.07-0066.
30. Chiang B, Kim YC, Doty AC, Grossniklaus HE, Schwendeman SP, Prausnitz MR. Sustained reduction of intraocular pressure by supraciliary delivery of brimonidine-loaded poly(lactic acid) microspheres for the treatment of glaucoma. *J Control Release*. 2016;228:48-57. doi:10.1016/j.jconrel.2016.02.041.
31. Kim YC, Edelhauser HF, Prausnitz MR. Targeted delivery of antiglaucoma drugs to the supraciliary space using microneedles. *Invest Ophthalmol Vis Sci*. 2014;55(11):7387-7397. doi:10.1167/iovs.14-14651.

32. Kim YC, Oh KH, Edelhauser HF, Prausnitz MR. Formulation to target delivery to the ciliary body and choroid via the suprachoroidal space of the eye using microneedles. *Eur J Pharm Biopharm.* 2015;95:398-406. doi:10.1016/j.ejpb.2015.05.020.
33. Chiang B, Venugopal N, Edelhauser HF, Prausnitz MR. Distribution of particles, small molecules and polymeric formulation excipients in the suprachoroidal space after microneedle injection. *Exp Eye Res.* 2016;153:101-109. doi:10.1016/j.exer.2016.10.011.
34. Noecker RJ, Herrygers LA, Anwaruddin R. Corneal and conjunctival changes caused by commonly used glaucoma medications. *Cornea.* 2004;23(5):490-496. doi:10.1097/01.ico.0000116526.57227.82.
35. Servat JJ, Bernardino CR. Effects of common topical antiglaucoma medications on the ocular surface, eyelids and periorbital tissue. *Drugs and Aging.* 2011;28(4):267-282. doi:10.2165/11588830-000000000-00000.
36. Baudouin C. Side effects of antiglaucomatous drugs on the ocular surface. *Curr Opin Ophthalmol.* 1996;7(2):80-86. <http://www.ncbi.nlm.nih.gov/pubmed/10163327>.
37. Caprioli J, Coleman AL. Intraocular pressure fluctuation: A risk factor for visual field progression at low intraocular pressures in the advanced glaucoma intervention study. *Ophthalmology.* 2008;115(7):1123-1129. doi:10.1016/j.ophtha.2007.10.031.
38. Ihekoromadu N, Lu F, Iwamura R, Yoneda K, Kawabata-Odani N, Shams NK. Safety and efficacy of DE-117, a selective EP₂ agonist in a phase 2a study. 2015;56:ARVO E-Abstract 5708.

39. Kirihara T, Iwamura R, Yoneda K, Kawabata-Odani N, Shimazaki A, Kawazu K. DE-117, a selective EP2 agonist, lowered intraocular pressure in animal models. 2015;56:ARVO E-Abstract 5709.
40. Lance KD, Good SD, Mendes TS, et al. In vitro and in vivo sustained zero-order delivery of rapamycin (sirolimus) from a biodegradable intraocular device. *Investig Ophthalmology Vis Sci.* 2015;56(12):7331-7337. doi:10.1167/iovs.15-17757.
41. Natu MV, Gaspar MN, Ribeiro CAF, et al. A poly(ϵ -caprolactone) device for sustained release of an anti-glaucoma drug. *Biomed Mater.* 2011;6(2):25003. doi:10.1088/1748-6041/6/2/025003.
42. Fialho SL, Behar-Cohen F, Silva-Cunha A. Dexamethasone-loaded poly(ϵ -caprolactone) intravitreal implants: A pilot study. *Eur J Pharm Biopharm.* 2008;68(3):637-646. doi:10.1016/j.ejpb.2007.08.004.
43. Silva-Cunha A, Fialho SL, Naud M-C, Behar-Cohen F. Poly- ϵ -caprolactone intravitreal devices: An in vivo study. *Investig Ophthalmology Vis Sci.* 2009;50(5):2312. doi:10.1167/iovs.08-2969.
44. Beeley NRF, Rossi JV, Mello-Filho PAA, et al. Fabrication, implantation, elution, and retrieval of a steroid-loaded polycaprolactone subretinal implant. *J Biomed Mater Res - Part A.* 2005;73(4):437-444. doi:10.1002/jbm.a.30294.
45. Bernards DA, Bhisitkul RB, Wynn P, et al. Ocular biocompatibility and structural integrity of micro- and nanostructured poly(caprolactone) films. *J Ocul Pharmacol Ther.* 2013;29(2):249-257. doi:10.1089/jop.2012.0152.

46. Schlesinger E, Ciaccio N, Desai TA. Polycaprolactone thin-film drug delivery systems: Empirical and predictive models for device design. *Mater Sci Eng C*. 2015;57:232-239. doi:10.1016/j.msec.2015.07.027.
47. Tsai JC. A comprehensive perspective on patient adherence to topical glaucoma therapy. *Ophthalmology*. 2009;116(11):S30-S36. doi:10.1016/j.ophtha.2009.06.024.
48. Wang Y, Challa P, Epstein DL, Yuan F. Controlled release of ethacrynic acid from poly(lactide-co-glycolide) films for glaucoma treatment. *Biomaterials*. 2004;25(18):4279-4285. doi:10.1016/j.biomaterials.2003.10.075.
49. Alvarez LJ, Zamudio AC, Candia OA. Sildenafil stimulates aqueous humor turnover in rabbits. *Exp Eye Res*. 2013;111:67-70. doi:10.1016/j.exer.2013.03.016.
50. Pitt CG, Chasalow FI, Hibionada YM, Klimas DM, Park T, Carolina N. Aliphatic polyesters I. The degradation of poly(ϵ -caprolactone) in vivo. *J Appl Polym Sci*. 1981;26(11):3779-3787. doi:10.1002/app.1981.070261124.
51. Sun H, Mei L, Song C, Cui X, Wang P. The in vivo degradation, absorption and excretion of PCL-based implant. *Biomaterials*. 2006;27(9):1735-1740. doi:10.1016/j.biomaterials.2005.09.019.
52. Wang L, Ma W, Gross RA, McCarthy SP. Reactive compatibilization of biodegradable blends of poly(lactic acid) and poly(ϵ -caprolactone). *Polym Degrad Stab*. 1998;59(1-3):161-168. doi:10.1016/S0141-3910(97)00196-1.
53. Kim J, Kudisch M, Mudumba S, et al. Biocompatibility and pharmacokinetic analysis of an intracameral polycaprolactone drug delivery implant for glaucoma. *Investig Ophthalmology Vis Sci*. 2016;57(10):4341-4346. doi:10.1167/iovs.16-19585.

54. Foo RCM, Lamoureux EL, Wong RCK, et al. Acceptance, attitudes, and beliefs of singaporean Chinese toward an ocular implant for glaucoma drug delivery. *Investig Ophthalmol Vis Sci.* 2012;53(13):8240-8245. doi:10.1167/iovs.12-10393.
55. Chan HH, Wong TT, Lamoureux E, Perera S. A survey on the preference of sustained glaucoma drug delivery systems by singaporean chinese patients: A comparison between subconjunctival, intracameral, and punctal plug routes. *J Glaucoma.* 2015;24(7):485-492. doi:10.1097/IJG.000000000000197.
56. Guerra FL, et al. In vitro hydrolysis of latanoprost by human ocular tissues. 2012;ARVO Abstract 5319/A344.
57. Mannermaa E, Vellonen KS, Urtti A. Drug transport in corneal epithelium and blood-retina barrier: Emerging role of transporters in ocular pharmacokinetics. *Adv Drug Deliv Rev.* 2006;58(11):1136-1163. doi:10.1016/j.addr.2006.07.024.
58. Urtti A, Pipkin JD, Rork G, Sendo T, Finne U, Repta AJ. Controlled drug delivery devices for experimental ocular studies with timolol 2. Ocular and systemic absorption in rabbits. *Int J Pharm.* 1990;61(3):241-249. doi:10.1016/0378-5173(90)90215-P.
59. Van Horn DL Van, Sendele DD, Seideman S, Bucu PJ. Regenerative capacity of the corneal endothelium in rabbit and cat. *Investig Ophthalmol Vis Sci.* 1977;16:597-613.
60. Van Horn DL, Hyndiuk RA. Endothelial wound repair in primate cornea. *Exp Eye Res.* 1975;21(2):113-124. doi:10.1016/0014-4835(75)90076-7.
61. Fechtner R, Realini T. Fixed combinations of glaucoma medications. *Curr Opin Ophthalmol.* 2004;15:132-135. doi:10.2298/SARH1510626B.
62. Sherwood MB, Craven ER, Chou C, DuBiner HB, et al. Twice-daily 0.2% brimonidine-0.5% timolol fixed-combination therapy vs monotherapy with timolol or

- brimonidine in patients with glaucoma or ocular hypertension. *Arch Ophthalmol.* 2006;124(9):1230-1238. doi:10.1001/archophth.124.9.1230.
63. Arici MK, Sayici M, Toker M, Erdogan H, Topalkara A. A short term study of the additive effect of timolol and brimonidine on intraocular pressure. *Eye (Lond).* 2002;16(1):39-43. doi:10.1038/sj.eye.6700035.
64. Cox JA, Mollan SP, Bankart J, Robinson R. Efficacy of antiglaucoma fixed combination therapy versus unfixed components in reducing intraocular pressure: a systematic review. *Br J Ophthalmol.* 2008;92(6):729-734. doi:10.1136/bjo.2008.139329.
65. Quaranta L, Biagioli E, Riva I, et al. Prostaglandin analogs and timolol-fixed versus unfixed combinations or monotherapy for open-angle glaucoma: a systematic review and meta-analysis. *J Ocul Pharmacol Ther.* 2013;29(4):382-389. doi:10.1089/jop.2012.0186.
66. Hoyng PF, van Beek LM. Pharmacological therapy for glaucoma: a review. *Drugs.* 2000;59(3):411-434. doi:10.2165/00003495-200059030-00003.
67. Rao R. Physiology of aqueous humor & factors maintaining normal IOP website. <https://www.slideshare.net/RohitRao2/physiology-of-aqueous-humor>. Accessed June 5, 2017.
68. Vareilles P, Silverstone D, Plazonnet B, Douarec J Le, Sears ML, Stone CA. Comparison of the effects of timolol and other adrenergic agents on intraocular pressure in the rabbit. *Invest Ophthalmol Vis Sci.* 1977;16(11):987-996.
69. Gregory DS. Timolol reduces IOP in normal NZW rabbits during the dark only. *Invest Ophthalmol Vis Sci.* 1990;31(4):715-721.

70. Maehara S, Ono K, Ito N, et al. Effects of topical nipradilol and timolol maleate on intraocular pressure, facility of outflow, arterial blood pressure and pulse rate in dogs. *Vet Ophthalmol.* 2004;7(3):147-150. doi:10.1111/j.1463-5224.2004.04010.x.
71. Takiyama N, Shoji S, Habata I, Ohba S. The effects of a timolol maleate gel-forming solution on normotensive beagle dogs. *J Vet Med Sci.* 2006;68(6):631-633.
72. Williams JM, Adewunmi A, Schek RM, et al. Bone tissue engineering using polycaprolactone scaffolds fabricated via selective laser sintering. *Biomaterials.* 2005;26(23):4817-4827. doi:10.1016/j.biomaterials.2004.11.057.
73. Coombes AGA, Rizzi SC, Williamson M, Barralet JE, Downes S, Wallace WA. Precipitation casting of polycaprolactone for applications in tissue engineering and drug delivery. *Biomaterials.* 2004;25(2):315-325. doi:10.1016/S0142-9612(03)00535-0.
74. Yeong WY, Sudarmadji N, Yu HY, et al. Porous polycaprolactone scaffold for cardiac tissue engineering fabricated by selective laser sintering. *Acta Biomater.* 2010;6(6):2028-2034. doi:10.1016/j.actbio.2009.12.033.
75. Liu SJ, Chiang FJ, Hsiao CY, Kau YC, Liu KS. Fabrication of balloon-expandable self-lock drug-eluting polycaprolactone stents using micro-injection molding and spray coating techniques. *Ann Biomed Eng.* 2010;38(10):3185-3194. doi:10.1007/s10439-010-0075-6.
76. Liu SJ, Hsiao CY, Chen JK, Liu KS, Lee CH. In-vitro release of anti-proliferative paclitaxel from novel balloon-expandable polycaprolactone stents. *Mater Sci Eng C.* 2011;31(5):1129-1135. doi:10.1016/j.msec.2011.04.011.

77. Guerra AJ, Farjas J, Ciurana J. Fibre laser cutting of polycaprolactone sheet for stents manufacturing : A feasibility study. *Opt Laser Technol.* 2017;95:113-123.
doi:10.1016/j.optlastec.2017.03.048.
78. Serrano MC, Pagani R, Vallet-Regí M, et al. In vitro biocompatibility assessment of poly(ϵ -caprolactone) films using L929 mouse fibroblasts. *Biomaterials.* 2004;25(25):5603-5611. doi:10.1016/j.biomaterials.2004.01.037.
79. Tang ZG, Black RA., Curran JM, Hunt JA, Rhodes NP, Williams DF. Surface properties and biocompatibility of solvent-cast poly(ϵ -caprolactone) films. *Biomaterials.* 2004;25(19):4741-4748. doi:10.1016/j.biomaterials.2003.12.003.
80. Lam CXF, Hutmacher DW, Schantz J-T, Woodruff MA, Teoh SH. Evaluation of polycaprolactone scaffold degradation for 6 months in vitro and in vivo. *J Biomed Mater Res A.* 2009;90(3):906-919. doi:10.1002/jbm.a.32052.
81. Rodriguez, F, Cohen C, Ober CK, Archer L. *Principles of polymer systems.* Boca Raton: CRC Press; 2015.
82. Sarasam A, Madihally S V. Characterization of chitosan-polycaprolactone blends for tissue engineering applications. *Biomaterials.* 2005;26(27):5500-5508.
doi:10.1016/j.biomaterials.2005.01.071.
83. Averous L, Moro L, Dole P, Fringant C. Properties of thermoplastic blends: Starch-polycaprolactone. *Polymer (Guildf).* 2000;41(11):4157-4167. doi:10.1016/S0032-3861(99)00636-9.
84. Sarazin P, Li G, Orts WJ, Favis BD. Binary and ternary blends of polylactide, polycaprolactone and thermoplastic starch. *Polymer (Guildf).* 2008;49(2):599-609.
doi:10.1016/j.polymer.2007.11.029.

85. Vadhar P, Kyu T. Effects of mixing on morphology, rheology, and mechanical properties of blends of ultra-high molecular weight polyethylene with linear low-density polyethylene. *Polym Eng Sci.* 1987;27(3):202-210.
doi:10.1002/pen.760270305.
86. Bodmeier R, Oh K, Chen H. The effect of the addition of low molecular weight poly (DL-lactide) on drug release from biodegradable poly (DL-lactide) drug delivery systems. *Int J Pharm.* 1989;51(1):1-8. doi:10.1016/0378-5173(89)90068-9.
87. Liggins RT, Burt HM. Paclitaxel-loaded poly(L-lactic acid) microspheres 3: Blending low and high molecular weight polymers to control morphology and drug release. *Int J Pharm.* 2004;282(1-2):61-71. doi:10.1016/j.ijpharm.2004.05.026.
88. Schindler A, Hibionada YM, Pitt CG. Aliphatic polyesters III. Molecular weight and molecular weight distribution in alcohol-initiated polymerizations of epsilon-caprolactone. *J Polym Sci Polym Chem Ed.* 1982;20:319-326.
doi:10.1002/pol.1982.170200206.
89. Eshraghi S, Das S. Mechanical & Microstructural properties of PCL scaffolds with 1-D, 2-D & 3-D orthogonally oriented porous architectures produced by selective laser sintering. *Acta Biomater.* 2011;6(7):2467-2476.
doi:10.1016/j.actbio.2010.02.002.Mechanical.

Publishing Agreement

It is the policy of the University to encourage the distribution of all theses, dissertations, and manuscripts. Copies of all UCSF theses, dissertations, and manuscripts will be routed to the library via the Graduate Division. The library will make all theses, dissertations, and manuscripts accessible to the public and will preserve these to the best of their abilities, in perpetuity.

Please sign the following statement:

I hereby grant permission to the Graduate Division of the University of California, San Francisco to release copies of my thesis, dissertation, or manuscript to the Campus Library to provide access and preservation, in whole or in part, in perpetuity.

Jean Kim
Author Signature

6/8/2017
Date